

Investigation of double hypernuclei production in Au+Au collisions around 3 GeV energies

Nihal Buyukcizmeci

Department of Physics, Selcuk University, Konya, Türkiye

(collaboration with A. Botvina, T. Reichert and M. Bleicher)

10th International Symposium on Non-equilibrium Dynamics

(NeD-2024)

25-29 November, 2024

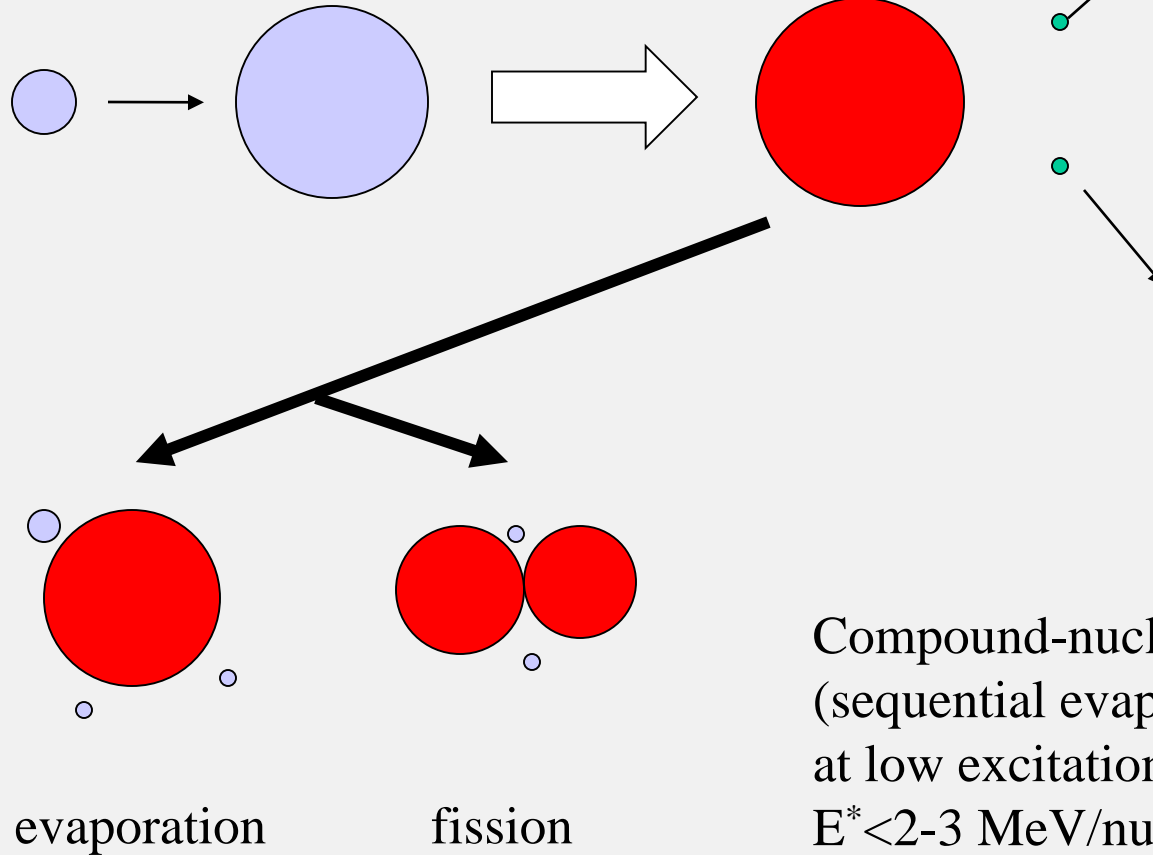
We acknowledge the Scientific and Technological Research Council of Türkiye (TUBITAK) support under Project No.124N105 and German Academic Exchange Service (DAAD) support from a PPP Exchange grant. N.B. thanks to conference support of Selcuk University BAP under Project Number 24701149.

Low/intermediate energies: hadron/lepton collisions with nuclei (+ peripheral ion collisions), the compound mechanism.

Dynamical stage with particle emission and production of excited nuclear residues

Preequilibrium emission + equilibration

Collective many-body process of nucleosynthesis

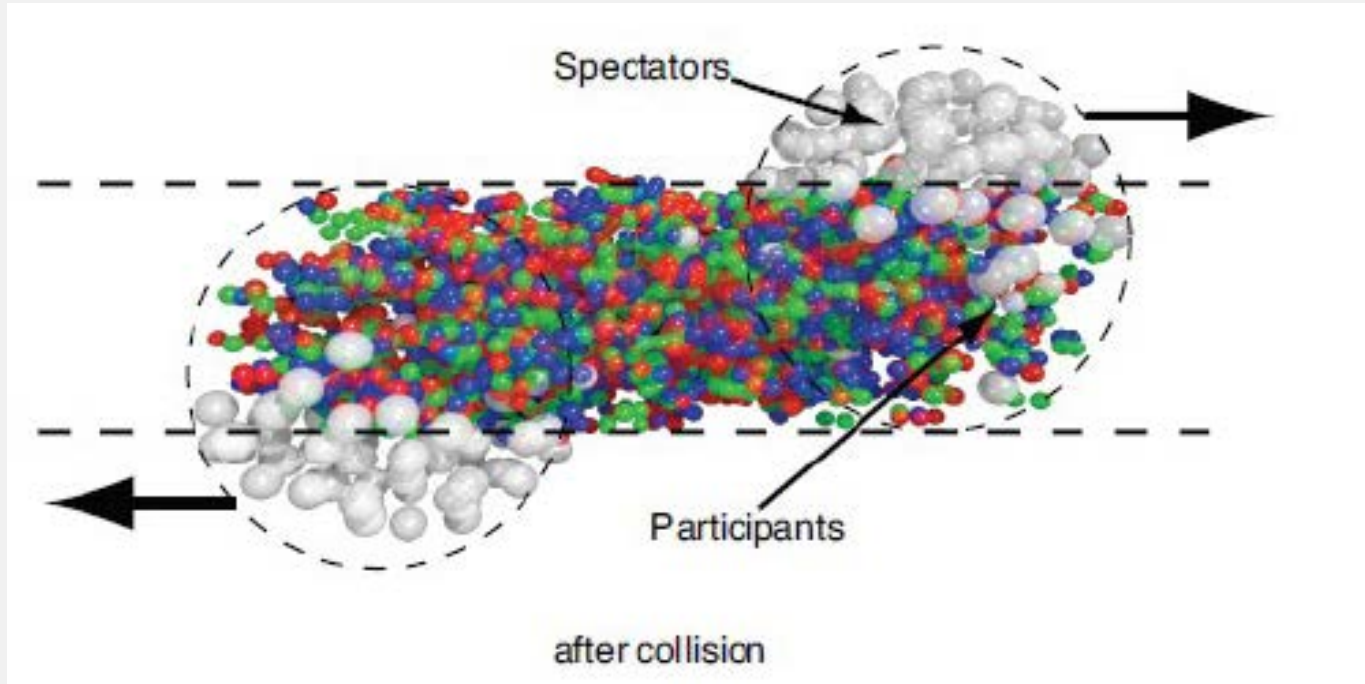


Statistical approach
N.Bohr (1936)

N.Bohr, J.Wheeler (1939)
V.Weisskopf (1937) ...

Compound-nucleus decay channels
(sequential evaporation or fission) dominate
at low excitation energy of thermal sources
 $E^* < 2-3 \text{ MeV/nucleon}$

Qualitative picture of dynamical stage of the
reaction leading to fragment production
(e.g., UrQMD calculations)



Very high energy is deposited into the nuclear system.
Compound nucleus conception may not work.
Fragment formation is possible from both participant nucleons and spectators

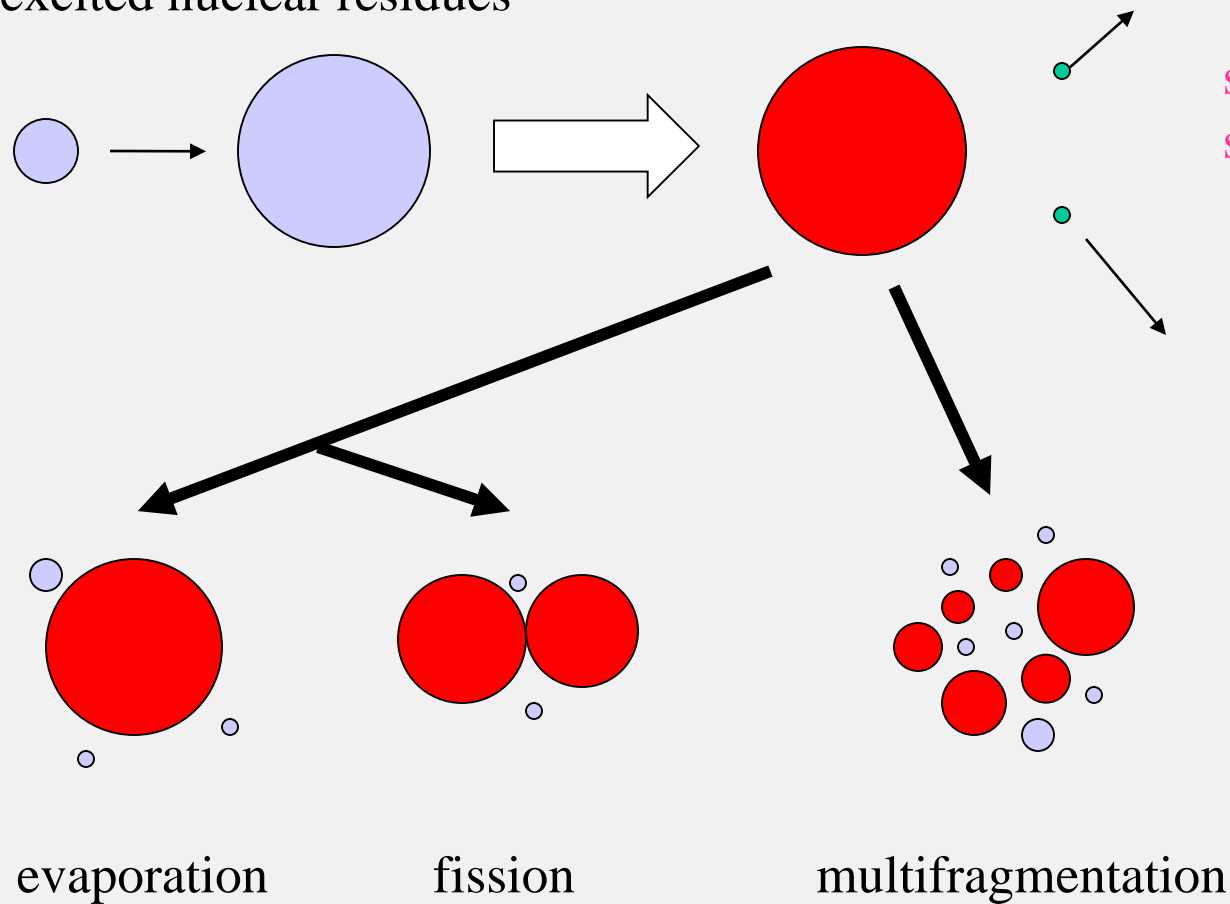


High excitation energy: New collective process – expansion of matter + nucleation/multifragmentation in the freeze-out state

Dynamical stage with particle emission and production of excited nuclear residues

Preequilibrium emission + equilibration

Statistical approach

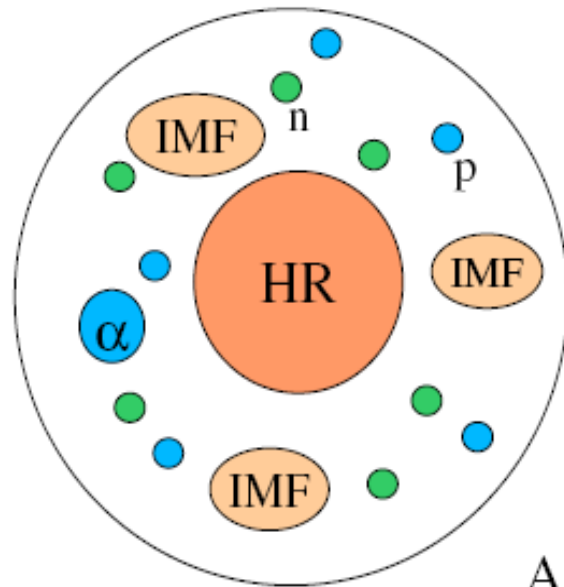


since 1980-th, conception:
statistical freeze-out volume

At high excitation energy $E^* > 3-4 \text{ MeV/nucleon}$ there is a simultaneous break-up into many fragments (e.g. microcanonical SMM: Phys.Rep.257(1995)133)

Statistical Multifragmentation Model (SMM)

J.P.Bondorf, A.S.Botvina, A.S.Iljinov, I.N.Mishustin, K.Sneppen, Phys. Rep. **257** (1995) 133



Ensemble of nucleons and fragments
in thermal equilibrium characterized by
neutron number N_0
proton number Z_0 , $N_0 + Z_0 = A_0$
excitation energy $E^* = E_0 - E_{CN}$
break-up volume $V = (1 + \kappa)V_0$ freeze-out

All break-up channels are enumerated by the sets
of fragment multiplicities or partitions, $f = \{N_{AZ}\}$

Statistical distribution of probabilities: $W_f \sim \exp \{S_f(A_0, Z_0, E^*, V)\}$
under conditions of baryon number (A), electric charge (Z) and energy
(E^*) conservation, including compound nucleus.

Statistical multifragmentation in central Au + Au collisions at 35 MeV/u

MINIBALL + MULTICS

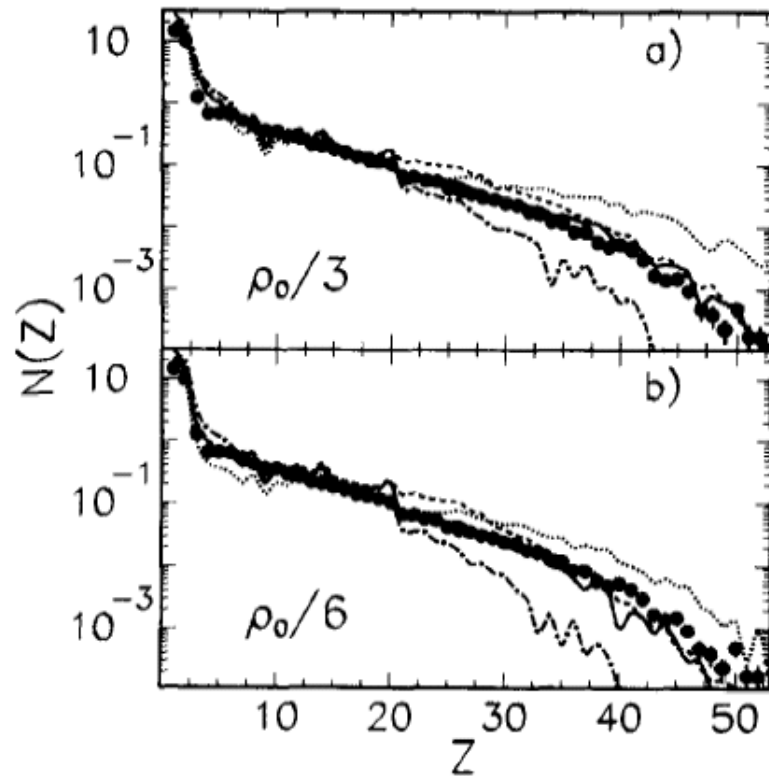


Fig. 1. Charge distribution $N(Z)$. Points show experimental data and lines show results of SMM predictions for sources with parameters $A_s = 343$, $Z_s = 138$, $E_s^*/A = 6.0$ MeV, $\rho_s = \rho_0/3$ (part a)) and $A_s = 315$, $Z_s = 126$, $E_s^*/A = 4.8$ MeV, $E_{\text{flow}}/A = 0.8$ MeV, $\rho_s = \rho_0/6$ (part b)). Dashed curves are the unfiltered calculations and solid curves are the filtered ones. The dot-dashed and dotted curves represent filtered calculations for thermal excitations $E_s^*/A + 1$ MeV/u and $E_s^*/A - 1$ MeV/u, respectively.

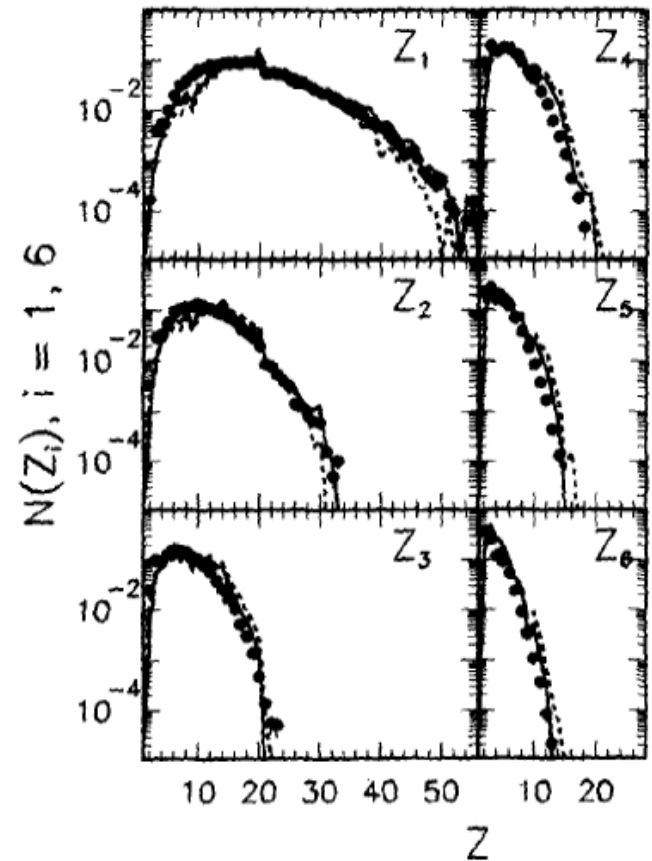


Fig. 2. Charge distribution of the six heaviest fragments, ordered such as $Z_i \geq Z_k$ if $i < k$. Experimental data are shown by points, the solid and dashed curves show the results of SMM calculations for $\rho_s = \rho_0/3$, and $\rho_s = \rho_0/6$, respectively (other source parameters as in Fig. 1).

Multifragmentation versus sequential evaporation

ISIS $\pi(8\text{GeV}/c)+\text{Au}$

ALADIN Au (600 MeV/n) + X.

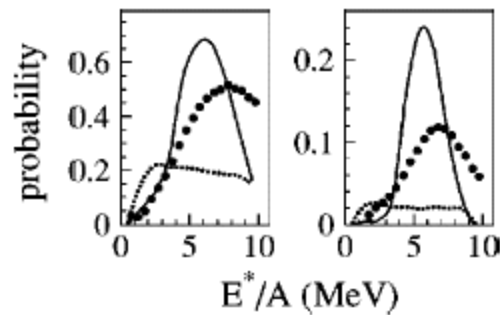


FIG. 3. Left panel: dots present the raw measured probability to detect an event with at least one heavy-fragment, $Z \geq 8$, and solid (dotted) line presents the SMM (GEMINI) model prediction filtered with the experimental detection efficiency. An initial angular momentum of $L=20\hbar$ for the hot nucleus was assumed for GEMINI model calculations. Right panel: as in left panel, but for the probability of detecting events with at least two heavy-fragments, $Z \geq 8$.

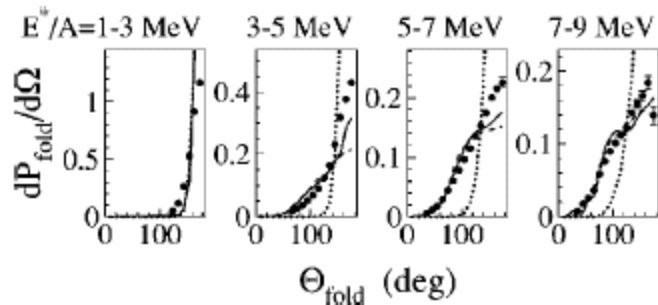


FIG. 2. The measured folding-angle (the angle between two $Z \geq 8$ fragments) probability for the indicated excitation-energy bins. Solid, dashed, and dotted lines show the SMM-hot, SMM-cold, and GEMINI model predictions, respectively, filtered with the experimental detection efficiency.

Nuclear Physics A556 (1993) 672-696

P. Kreuz et al. / Charge correlations

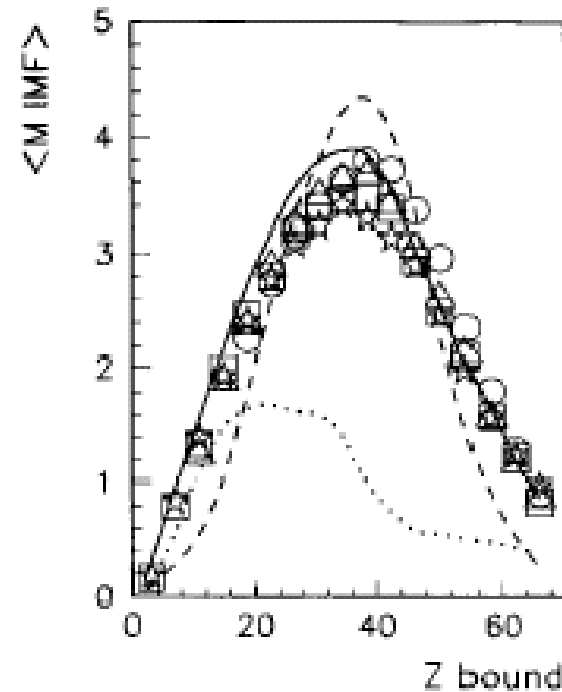


Fig. 15. The average multiplicity of IMFs as a function of Z_{bound} for Au 600 MeV/nucleon collisions on C (circles), Al (triangles), Cu (squares) and Pb (stars). The error bars are in most cases smaller than the size of the symbols. The lines are COPENHAGEN (dashed), GEMINI (dotted) and percolation (full) predictions.

Time scale of the thermal multifragmentation

angle correlations of fragments

p(8.1 GeV) + Au

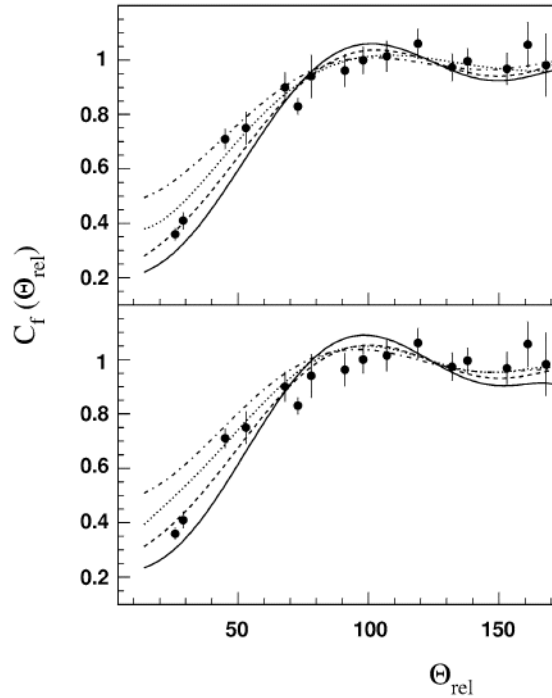


Fig. 5. Comparison of the measured correlation functions (full circles) with the calculated ones for different mean decay times of the fragmenting system: solid, dashed, dotted and dash-dotted lines for $\tau = 0, 50, 100$ and 200 fm/c. The upper panel is for the RC + α + SMM model with the parameters (4, 8, η) (see notation in Fig. 4), the lower panel is for the same model, but with the parameters (4, 4, η) allowing the fragments to overlap (see text).

FASA collaboration

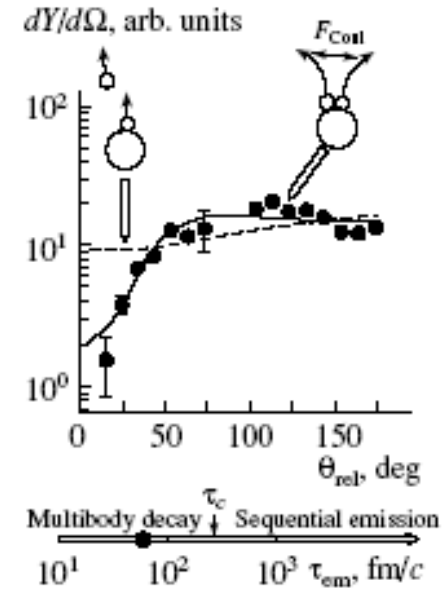
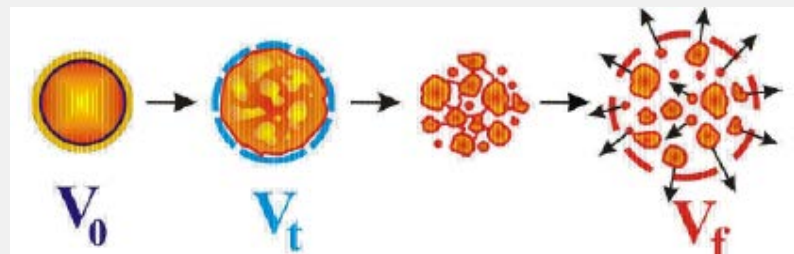


Fig. 5. Distribution of relative angles between coincident IMFs for ${}^4\text{He}$ (14.6 GeV) + Au collisions. The solid curve is calculated for the simultaneous emission of fragments; the dashed curve corresponds to the sequential, independent evaporation.



The formation of nuclear fragments in collisions of nuclei is a many-body process, there is no a dominating channel. The theoretical explanation requires both dynamical and statistical approaches.

It can be subdivided into two main stages:

- 1) Dynamical stage leading to the production of new baryons (+ in some cases, lightest nuclei) and to excited equilibrated nuclear systems, e.g., dense nuclear residues and baryonic clusters at the diluted density.**
- 2) Statistical disassembly of the systems consisting of produced baryons (including the nuclear residues/clusters), which leads to the production of final nuclei.**

UrQMD

PHSD

DCM

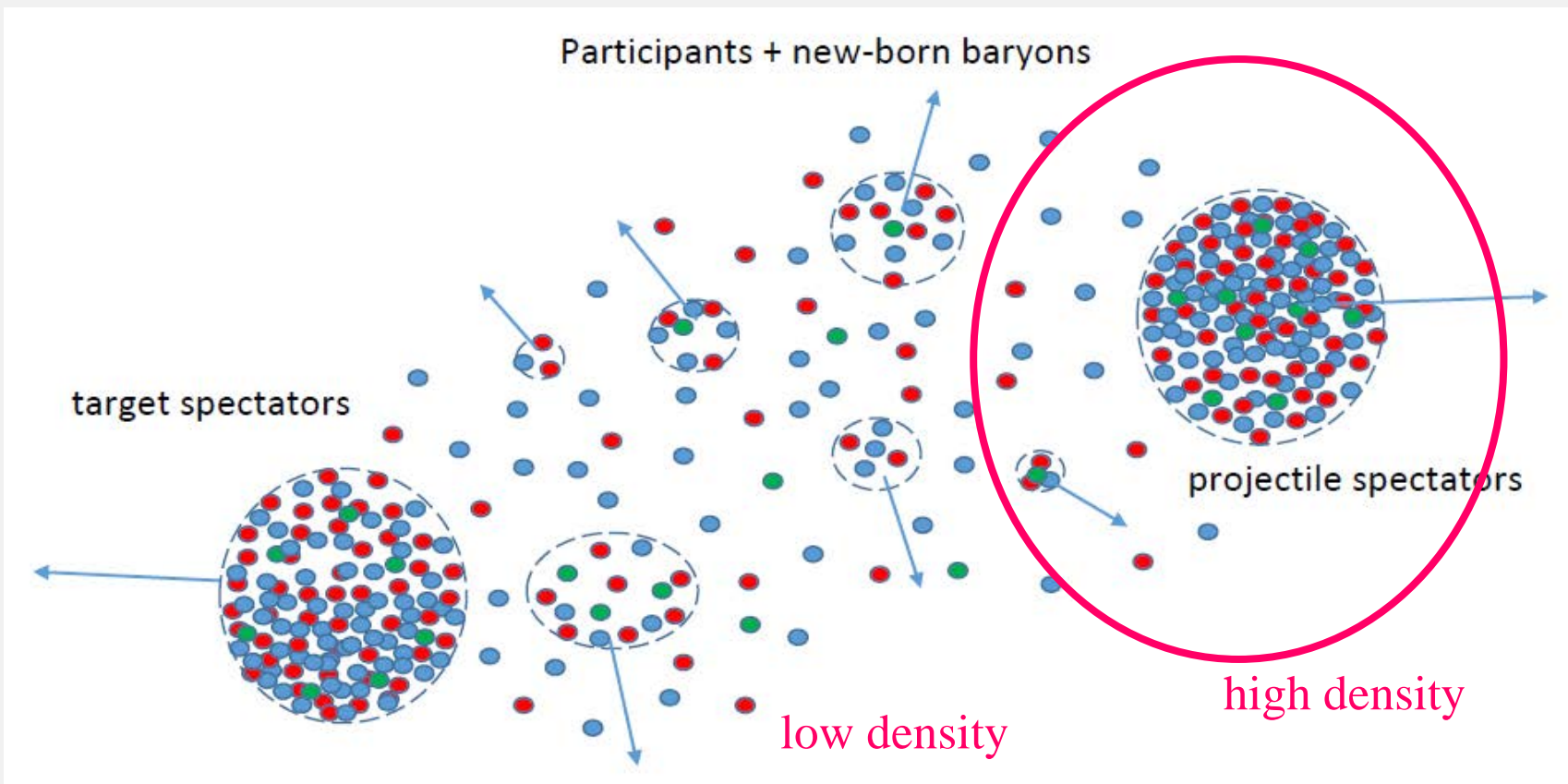
GiBUU

Production mechanisms of nuclear cluster species including anti-matter, hyper-matter in relativistic HI and hadron collisions:

- Production of all kind of particles (anti- , strange, charmed ones) in individual binary hadron collisions. Effects of nuclear medium can be included.
- Secondary interactions and rescattering of new-born particles are taken into account. (Looks as partial ‘thermalization’.)
- Stochastic separation (coalescent-like) of produced baryons into composite (normal. exotic, anti- , hyper-) nuclear species.
- Capture of produced baryons by big excited nuclear residues.

Statistical decay of excited nuclear species into final nuclei

- Multifragmentation into small nuclei (high excitations),
- Evaporation and fission of large nuclei (low excitations),
- (Fermi-) Break-up of small nuclei into lightest ones.



At sub-nuclear density: subdivision of matter into multiple clusters consisting of dynamically produced/spectator baryons, when baryons are close in the phase space (because of the remaining interaction).

The clusters are excited, and are in chemical equilibrium leading to the nucleation inside clusters. This case can be realized in Heavy-Ion collisions of medium/high energies.

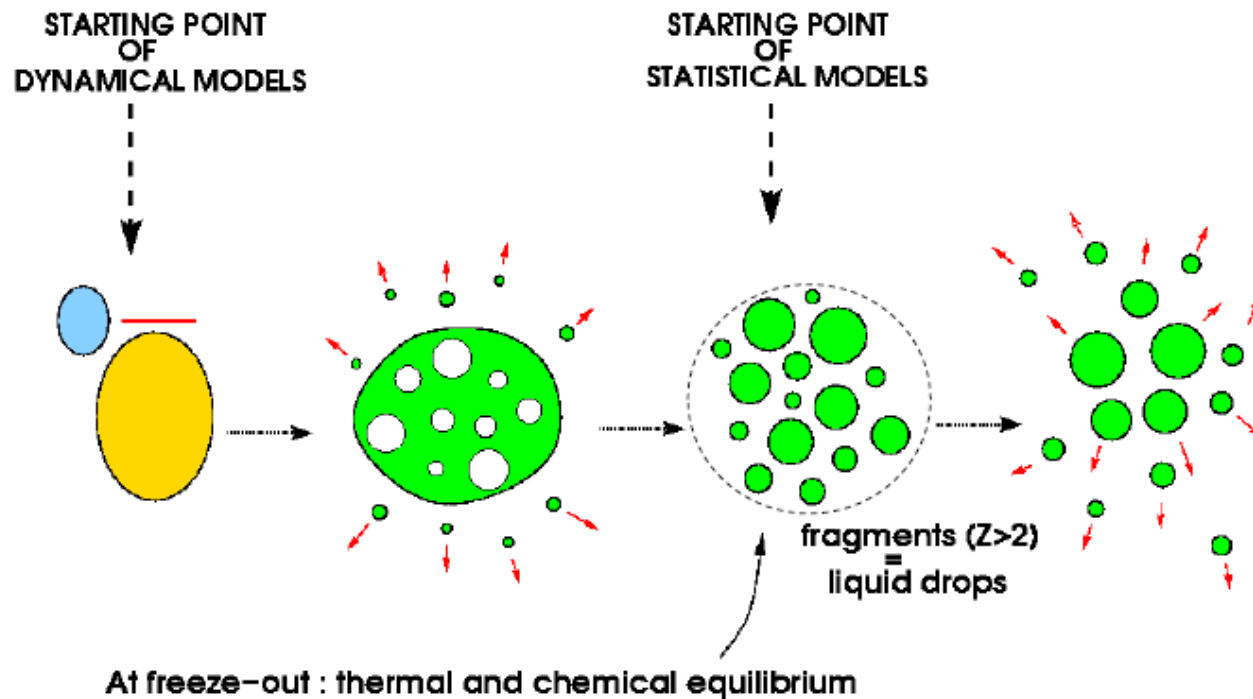
Production of large nuclear fragments in reaction initiated by high energy light particles and in peripheral nucleus-nucleus collisions:

Formation of excited nuclear residues (projectile/target) after the dynamical stage.

Multifragmentation in intermediate and high energy nuclear reactions

Experimentally established:

- 1) few stages of reactions leading to multifragmentation,
- 2) short time $\sim 100\text{fm}/c$ for primary fragment production,
- 3) freeze-out density is around $0.1\rho_0$,
- 4) high degree of equilibration at the freeze-out,
- 5) primary fragments are hot.



Two-stage multifragmentation of 1A GeV Kr, La, and Au

EOS collaboration: fragmentation of relativistic projectiles

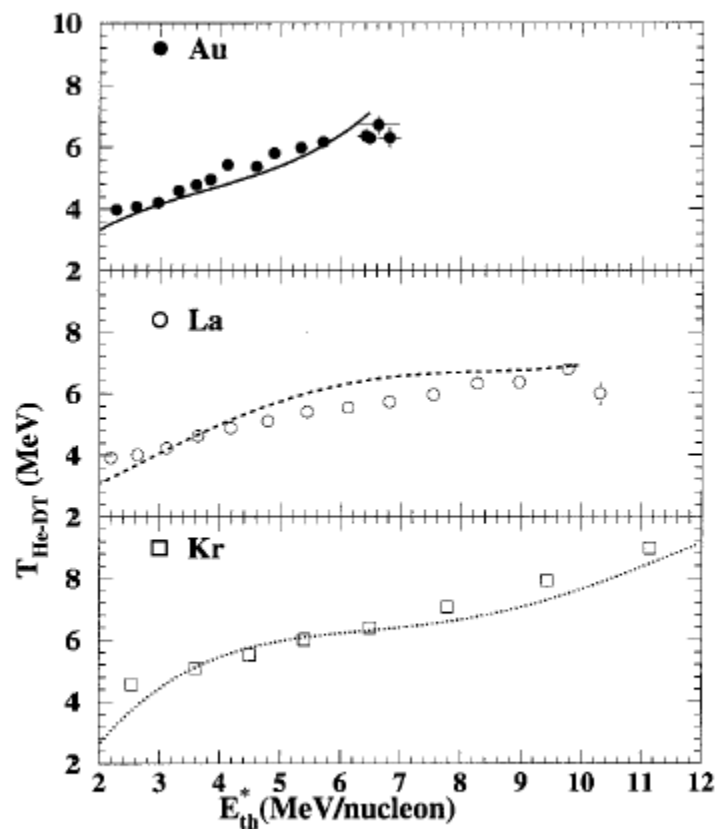


FIG. 19. Caloric curves (T_f vs E_{th}^*/A) for Kr, La, and Au. Points are experimental and curves are from SMM.

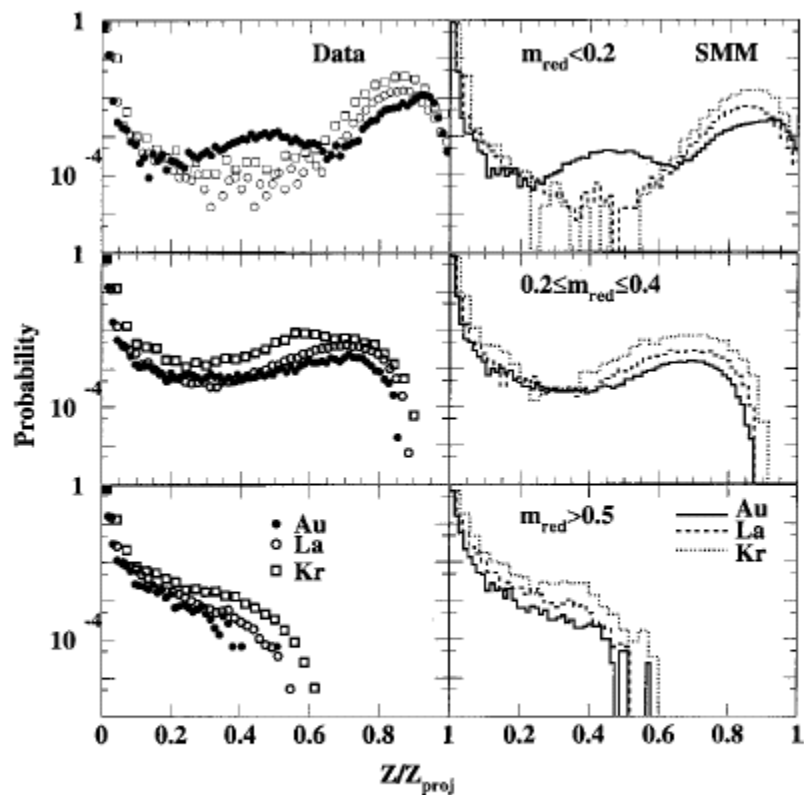
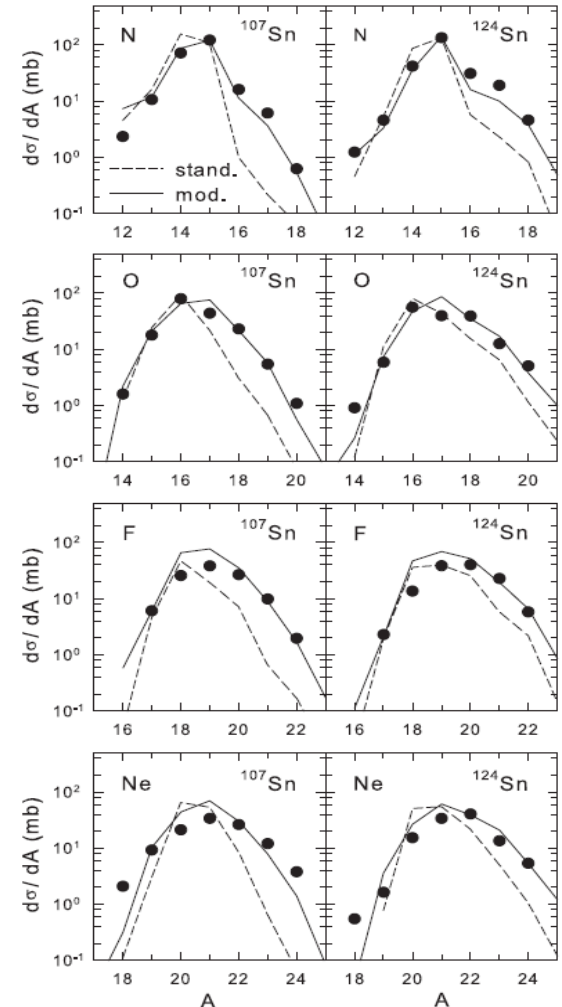
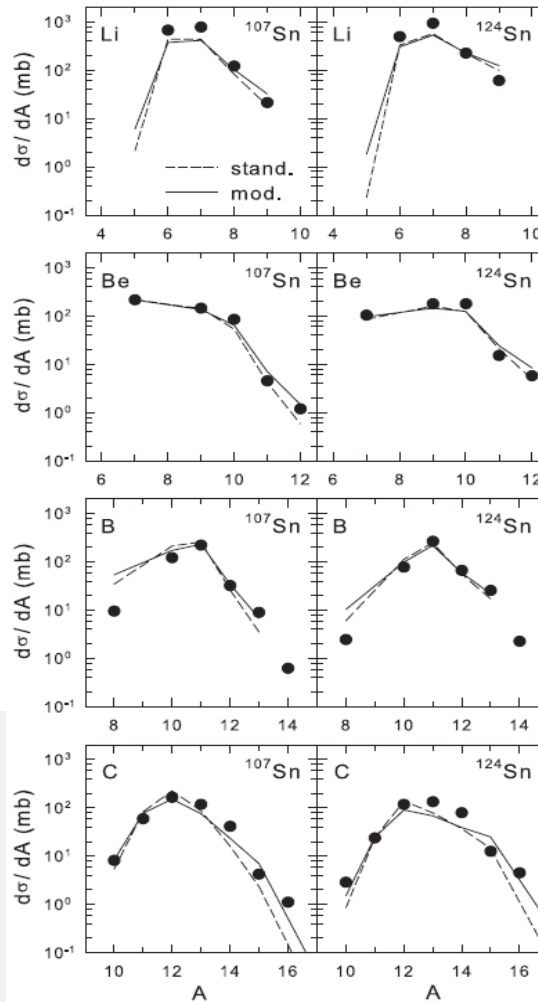
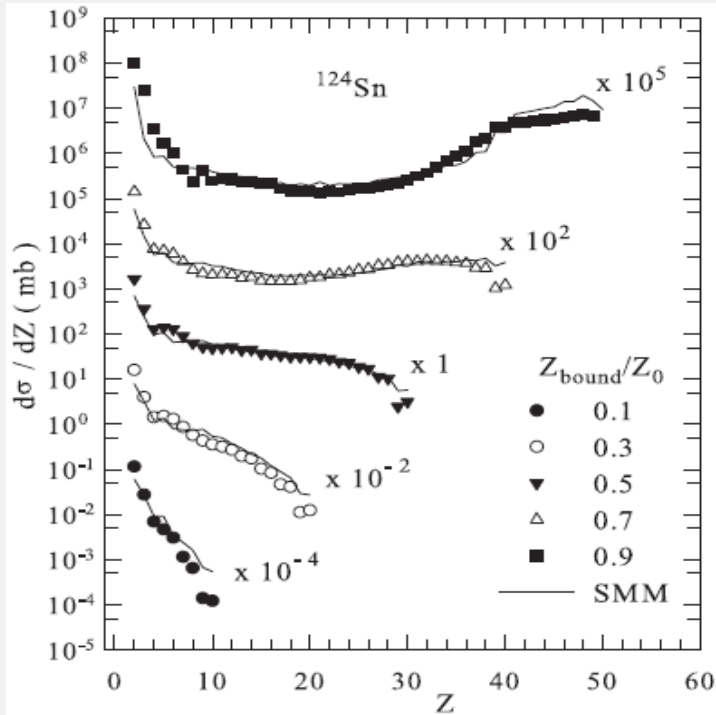


FIG. 24. Second stage fragment charge distribution as a function of $Z/Z_{\text{projectile}}$. Results are shown for three reduced multiplicity intervals for both data and SMM.

Isospin-dependent multifragmentation of relativistic projectiles

$^{124,107}\text{-Sn}$, $^{124}\text{-La}$ (600 A MeV) + Sn \rightarrow projectile (multi-)fragmentation

Very good description is obtained within Statistical Multifragmentation Model, including fragment charge yields, isotope yields, various fragment correlations.



Statistical (chemical) equilibrium is established at break-up of hot projectile residues ! In the case of strangeness admixture we expect it too !

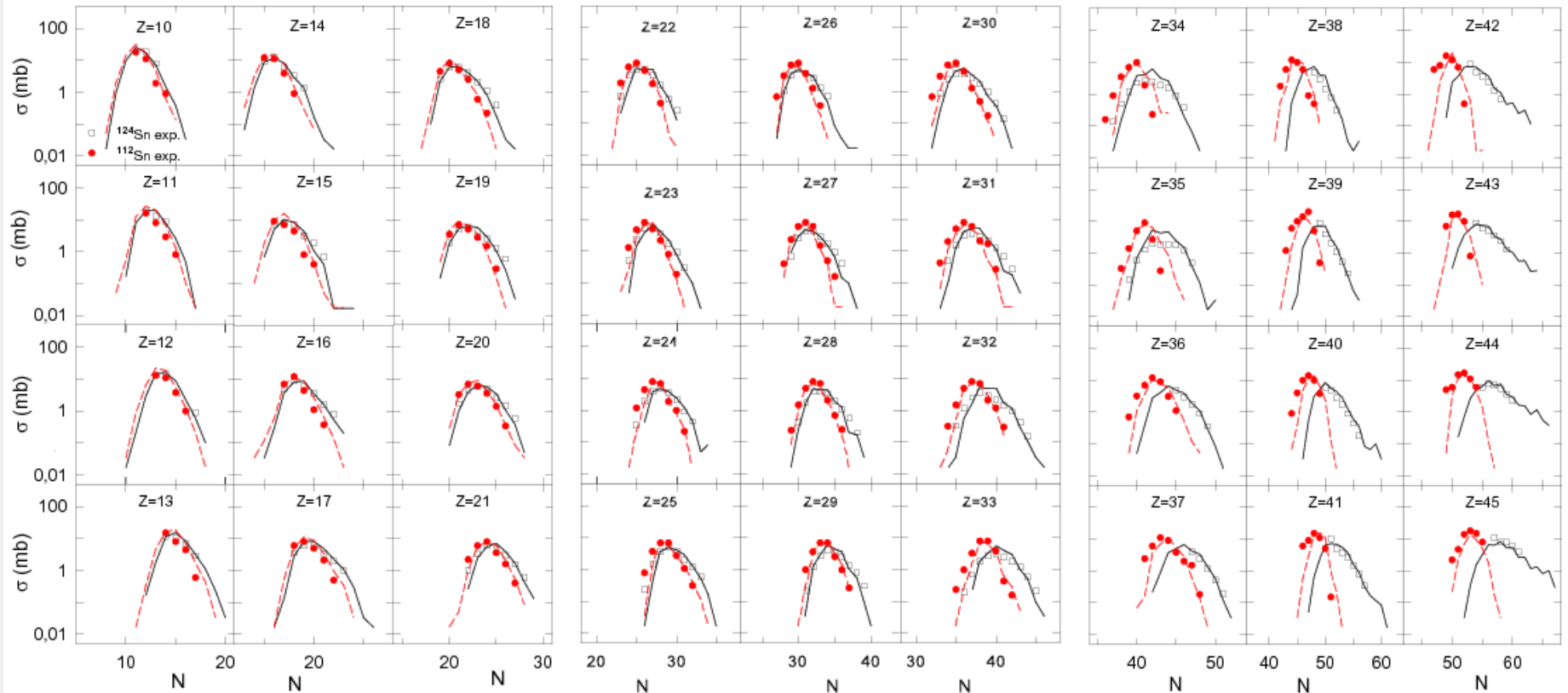
FRS data @ GSI

FRS projectile fragmentation of two symmetric systems $^{124}\text{Sn} + ^{124}\text{Sn}$ and $^{112}\text{Sn} + ^{112}\text{Sn}$ at an incident beam energy of 1 A GeV measured with high-resolution magnetic spectrometer FRS. (V. Föhr, et al., Phys. Rev. C **84**, (2011) 054605)

Experimental data are well reproduced with statistical calculations in the SMM-ensemble. To reproduce the FRS data symmetry energy term is reduced as shown in the table. We have also found a decreasing trend of the symmetry energy with increasing charge number, for the neutron-rich heavy fragments resulting from ^{124}Sn projectile.

H. Imal, A.Ergun, N. Buyukcizmeci, R.Ogul, A.S. Botvina, W. Trautmann, C **91**, 034605 (2015)

Z	^{112}Sn	^{124}Sn
interval	γ (MeV)	γ (MeV)
10-17	16	16
18-25	19	18
26-31	21	20
32-37	23	19
38-45	25	18



ALADIN data

GSI

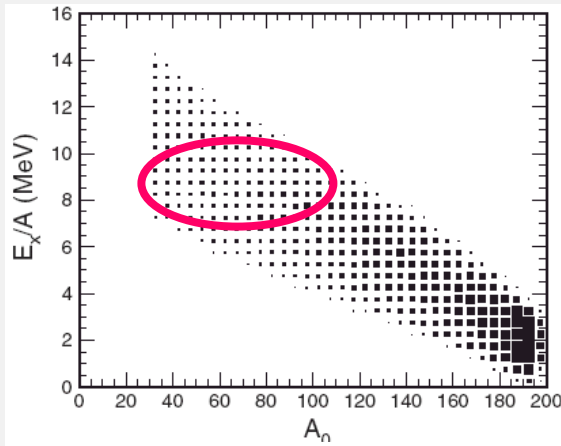
multifragmentation of relativistic projectiles

A.S.Botvina et al.,
Nucl.Phys. A584(1995)737

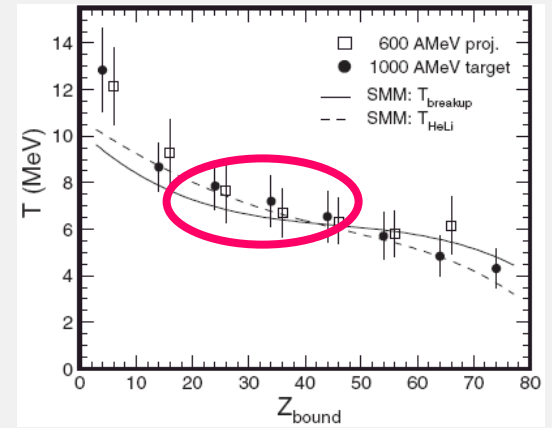
H.Xi et al.,
Z.Phys. A359(1997)397

comparison with
SMM (statistical
multifragmentation
model)

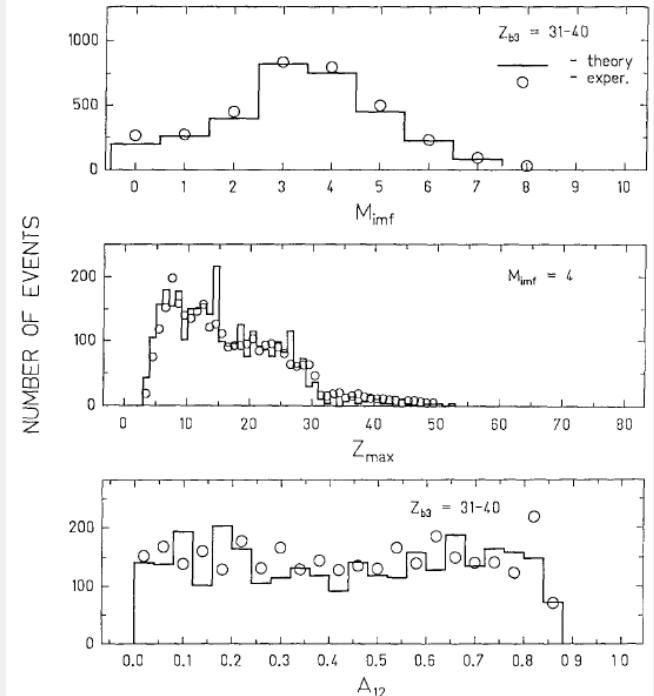
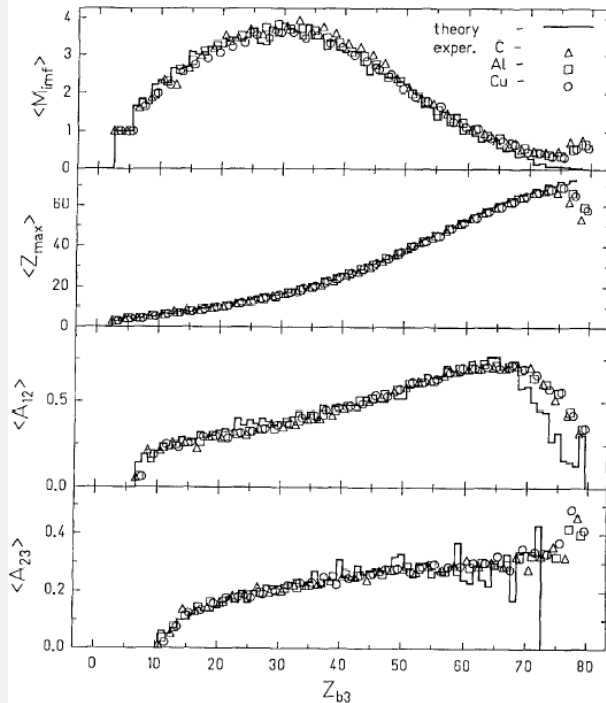
Statistical equilibrium
has been reached in
these reactions



Au(600MeV/n)+C,Al,Cu

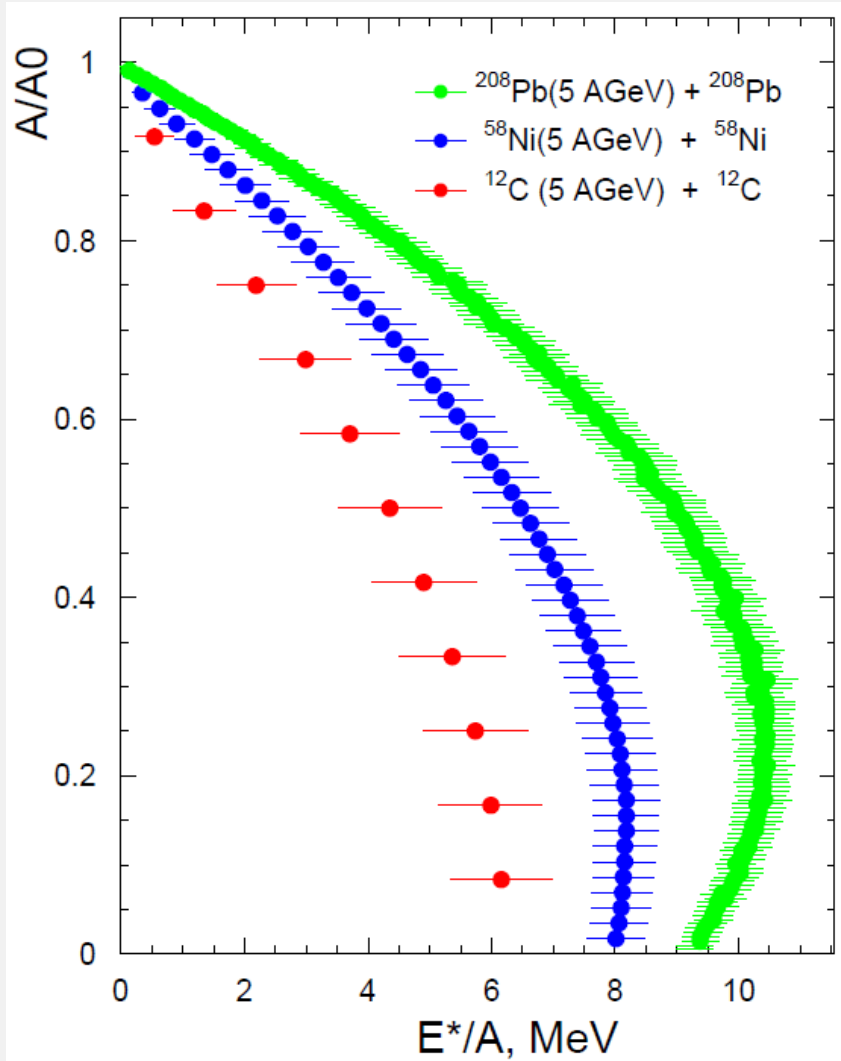


Au(600MeV/n)+Cu



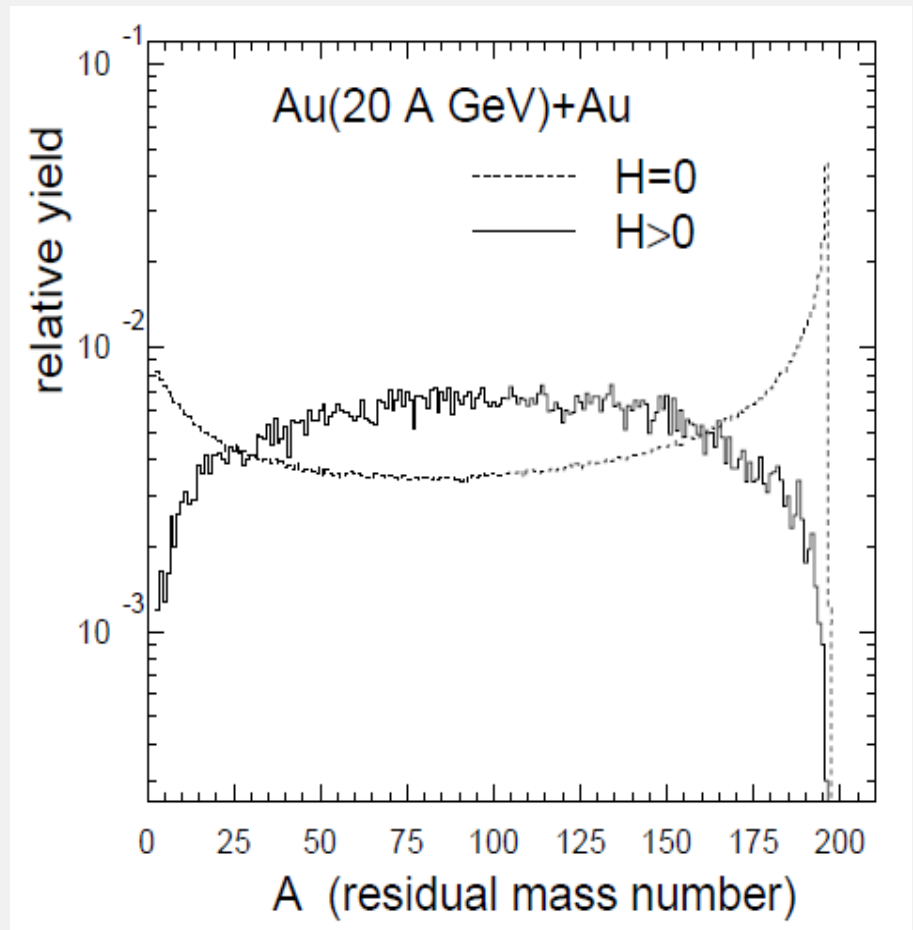
Excitation energies of the nuclear spectator residuals

DCM : PRC95, 014902 (2017)



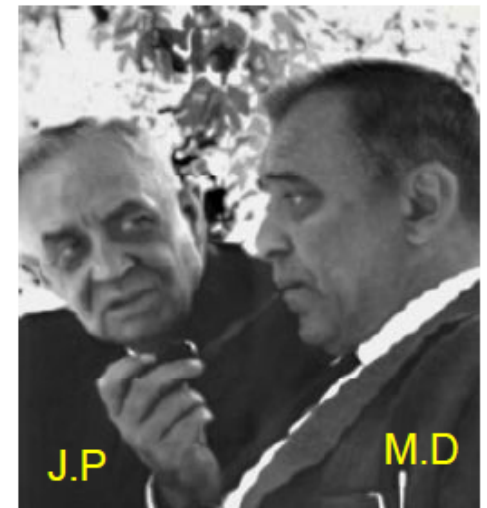
PRC84, 064904 (2011)

Masses of projectile residuals produced at dynamical stage (6b: $H=0$, 0.2b: $H>0$)



Discovery of a Strange nucleus: Hypernucleus

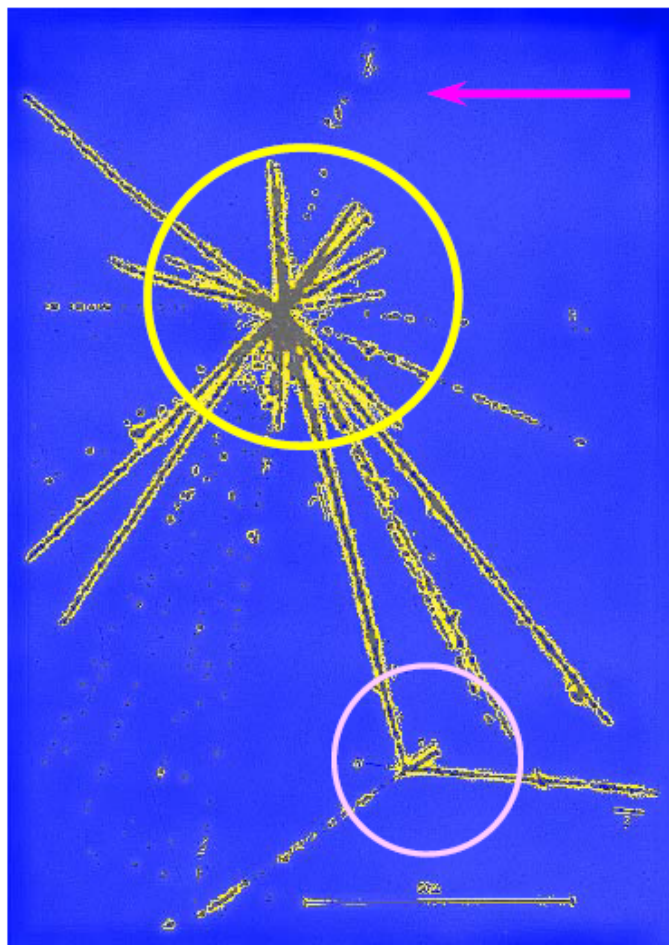
M. Danysz and J. Pniewski, *Philos. Mag.* 44 (1953) 348



J.P

M.D

First-hypernucleus was observed in a stack of photographic emulsions exposed to cosmic rays at about 26 km above the ground.



Incoming high energy proton from cosmic ray

colliding with a nucleus of the emulsion, breaks it in several fragments forming a star. **Multifragmentation !**

All nuclear fragments stop in the emulsion after a short path

From the first star, 21 Tracks => $9\alpha + 11H + 1_{\Lambda}X$

The fragment $_{\Lambda}X$ disintegrates later, makes the bottom star. Time taken $\sim 10^{-12}$ sec (typical for weak decay)

This particular nuclear fragment, and the others obtained afterwards in similar conditions, were called **hyperfragments or hypernuclei.**

$N_u \sim N_d \sim N_s$



$S = -\infty$

Strangeness in neutron stars ($\rho > 3 - 4 \rho_0$)

Strange hadronic matter ($A \rightarrow \infty$)

$p, n, \Lambda, \Xi^0, \Xi^-$

↑ higher density



p n

Strangeness

$S = -2$

$S = -1$

$\Lambda\Lambda, \Xi$ hypernuclei

Λ, Σ hypernuclei

ΛN interaction

Proton-rich nuclei

Neutron-rich nuclei

proton number

non-strange nuclei

neutron number



neutron halo

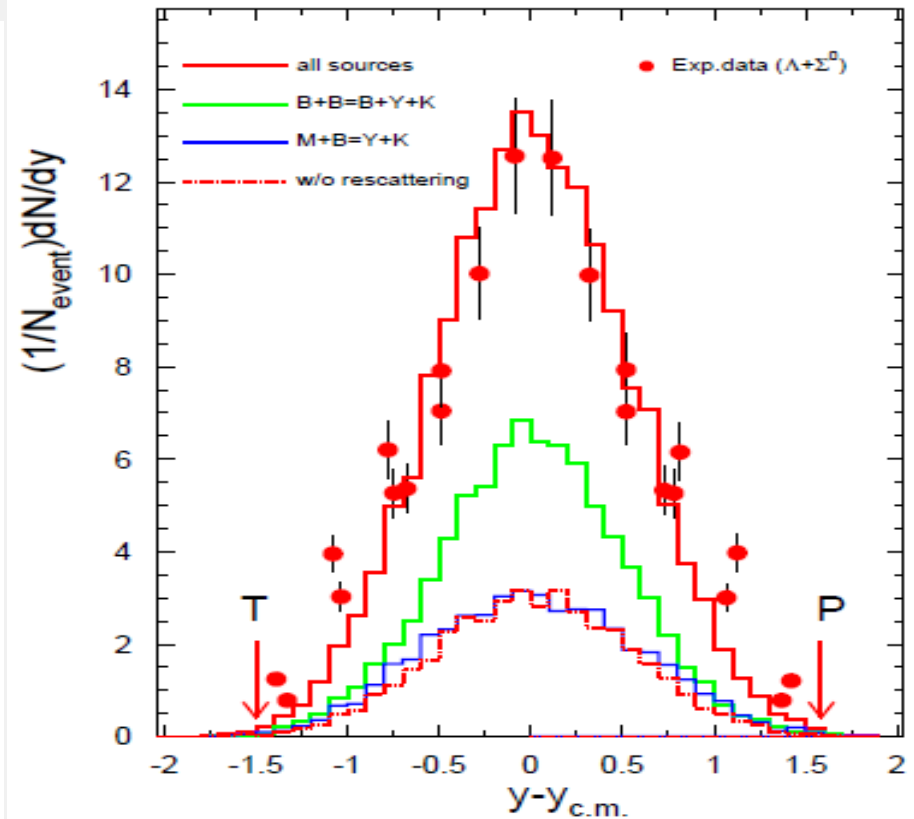
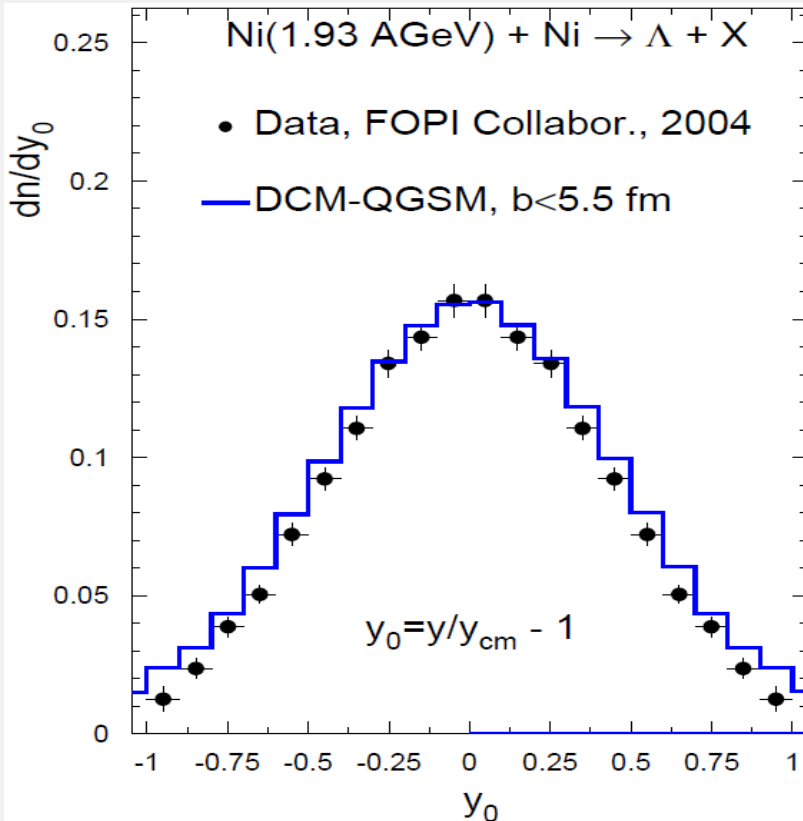
3-dimensional nuclear chart

All transport modes predict similar picture:
 baryons can be produced at all rapidities, in
 participant and spectator kinematic regions.

Wide rapidity distribution of
 produced Λ !

Calculation: DCM
 PRC84(2011)064904
 Au(11AGeV/c)+Au

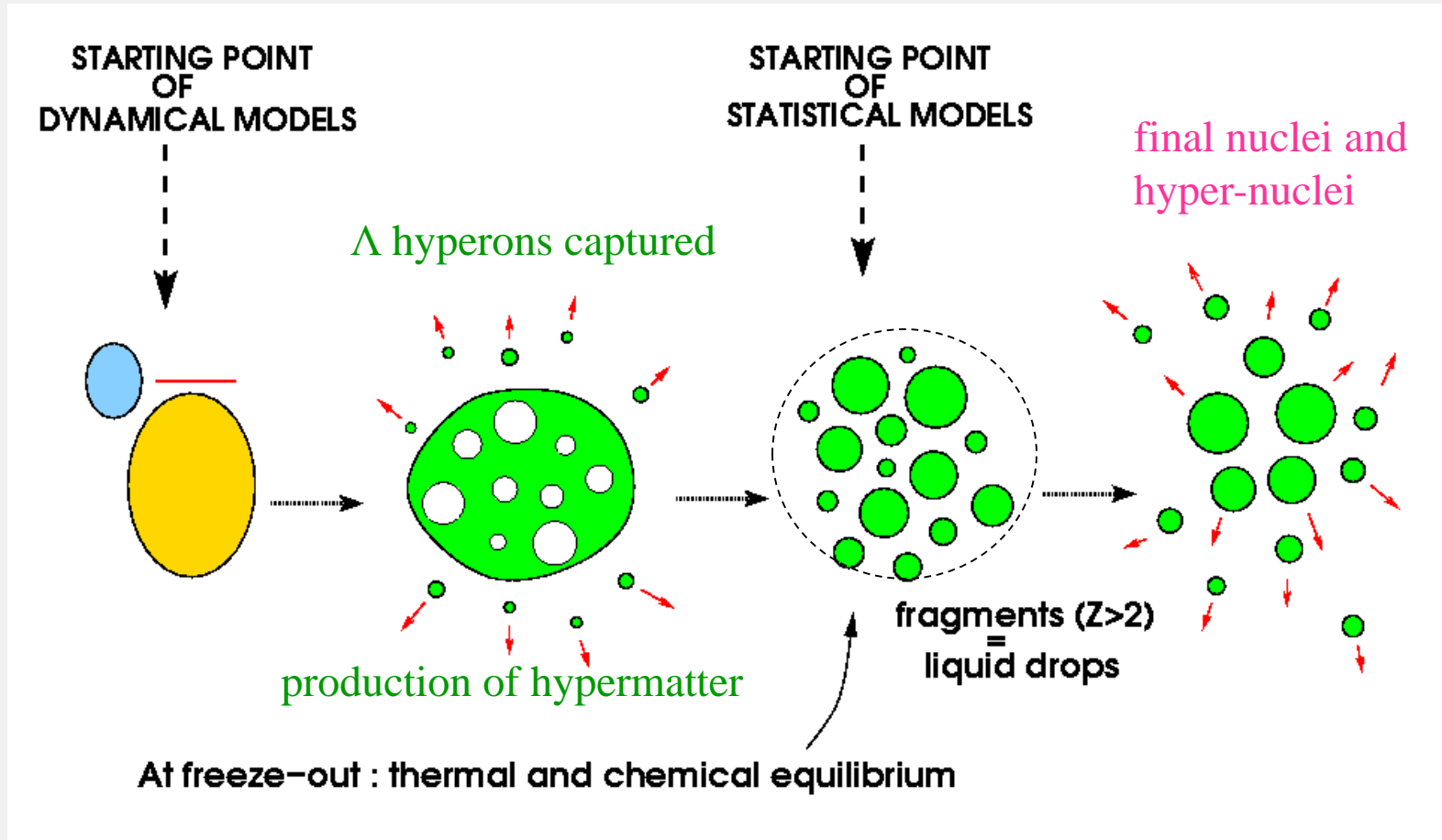
S.Albergo et al.,
 E896:
 PRL88(2002)062301



Generalization: statistical de-excitation model for nuclei with Lambda hyperons

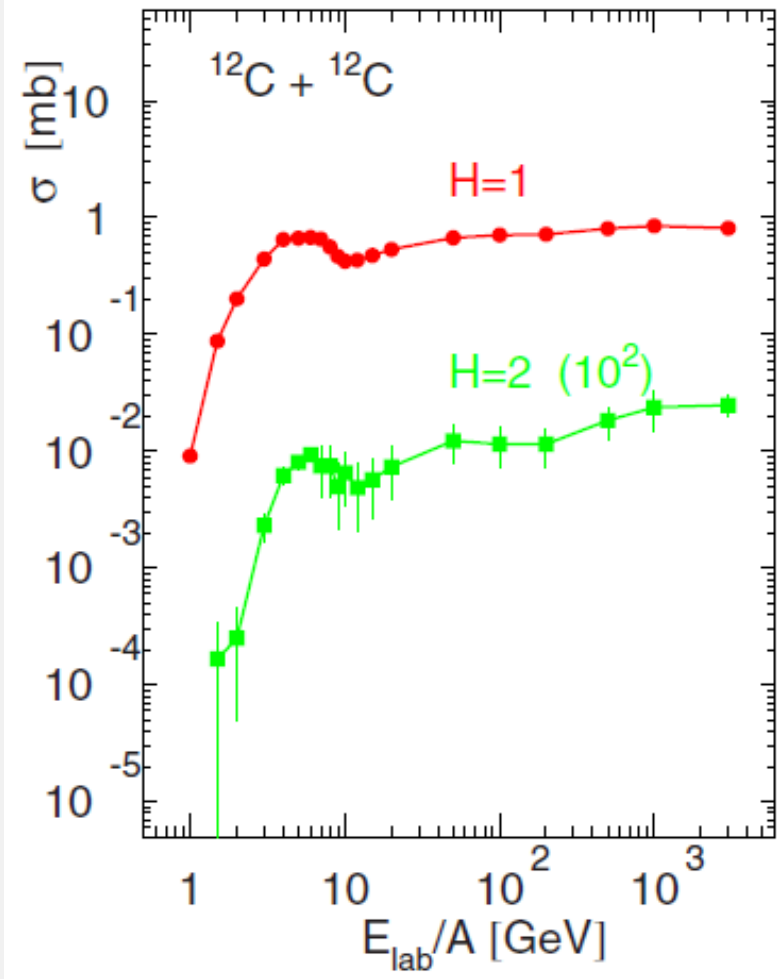
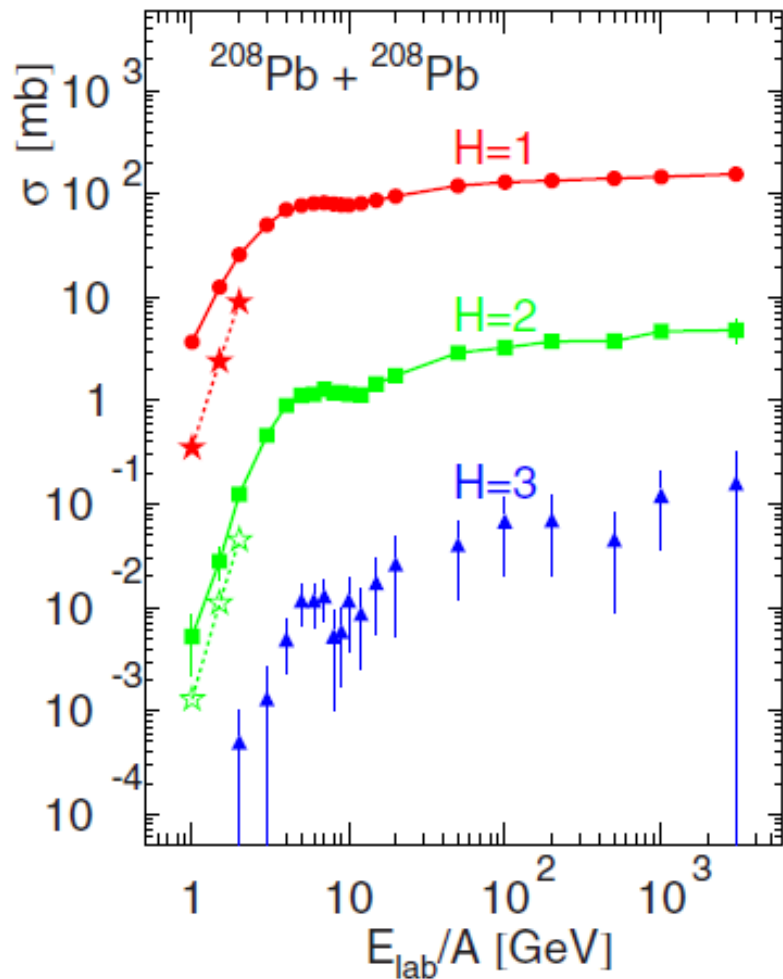
In these reactions we expect analogy with

multifragmentation in intermediate and high energy nuclear reactions
+ nuclear matter with strangeness

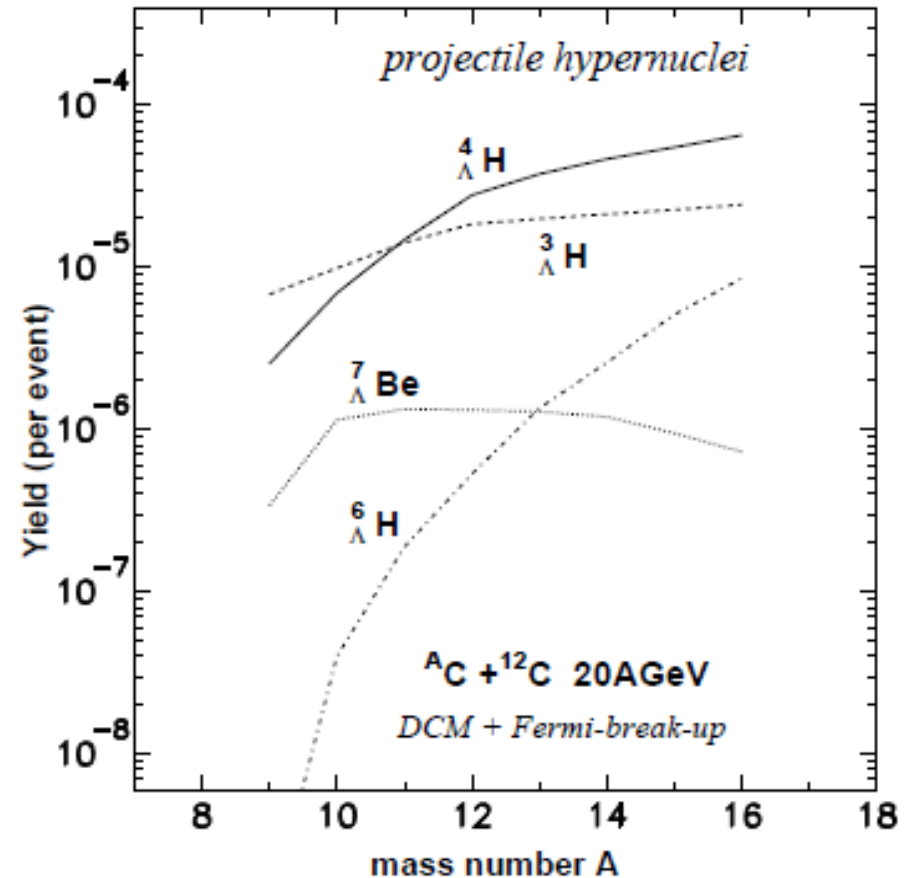
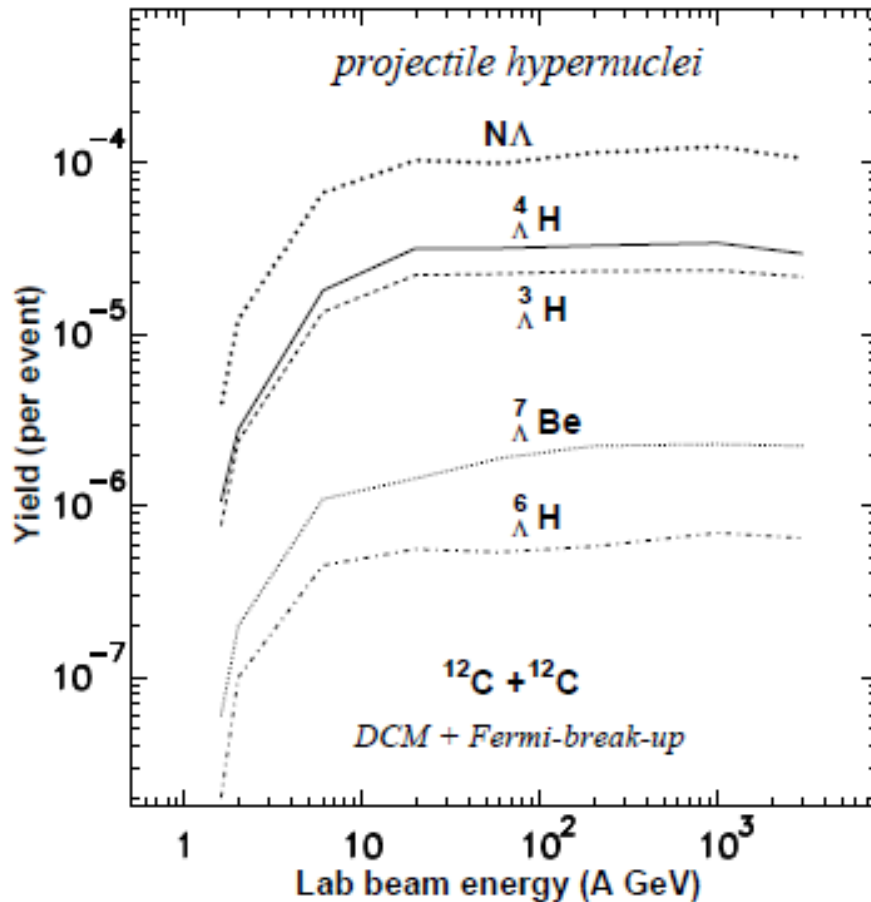


Production of excited hyper-residues in peripheral collisions, decaying into hypernuclei (target/projectile rapidity region).

DCM and UrQMD + CB predictions: Phys. Rev. C95, 014902 (2017)



Production of light hypernuclei in relativistic ion collisions



One can use exotic neutron-rich and neutron-poor projectiles, which are not possible to use as targets in traditional hyper-nuclear experiments, because of their short lifetime. Comparing yields of hypernuclei from various sources we can get info about their binding energies and properties of hyper-matter.

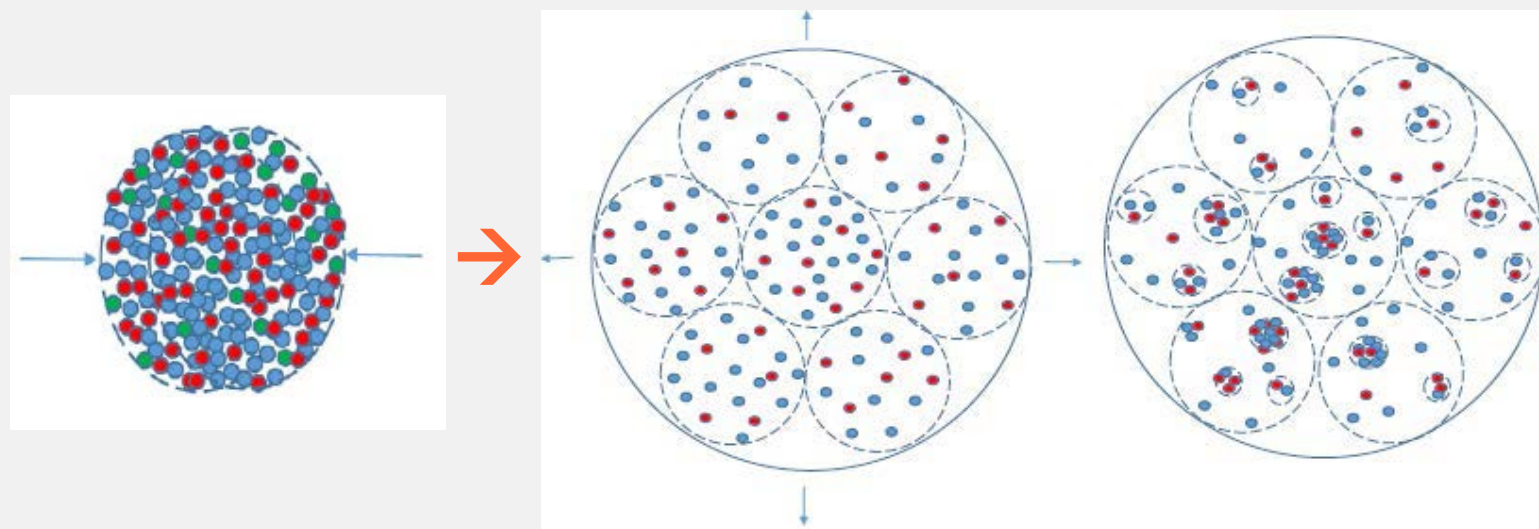
CENTRAL COLLISIONS: formation of excited isotropic nuclear matter

Nuclear system expands to low densities and passes the density around 0.1 of normal nuclear density, which corresponds to the freeze-out adopted in the statistical models. Baryons can still interact and form nuclei at this density. We divide the nuclear matter into clusters in local chemical equilibrium and apply SMM to describe the nucleation process in these clusters.

dynamical expansion
after collision/compress.

Baryonic clusters in
local equilibrium (freeze-out)

nuclei formation inside
the clusters - SMM



CENTRAL COLLISIONS: one can apply the special selection of events of nucleus-nucleus collisions (e.g., ERAT criterion in FOPI experiment). This selection can also require the special model application.

To describe the nuclei formation with controlled models:

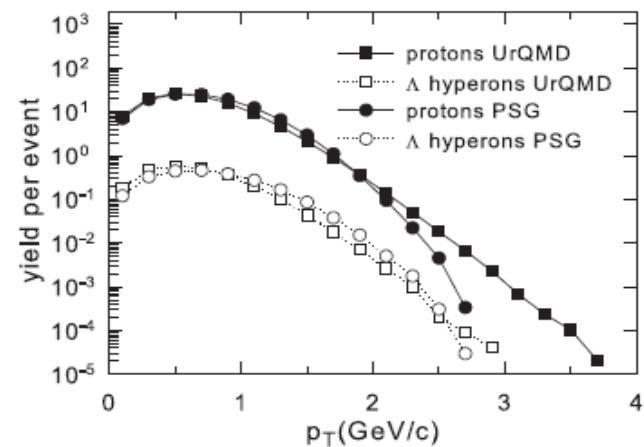
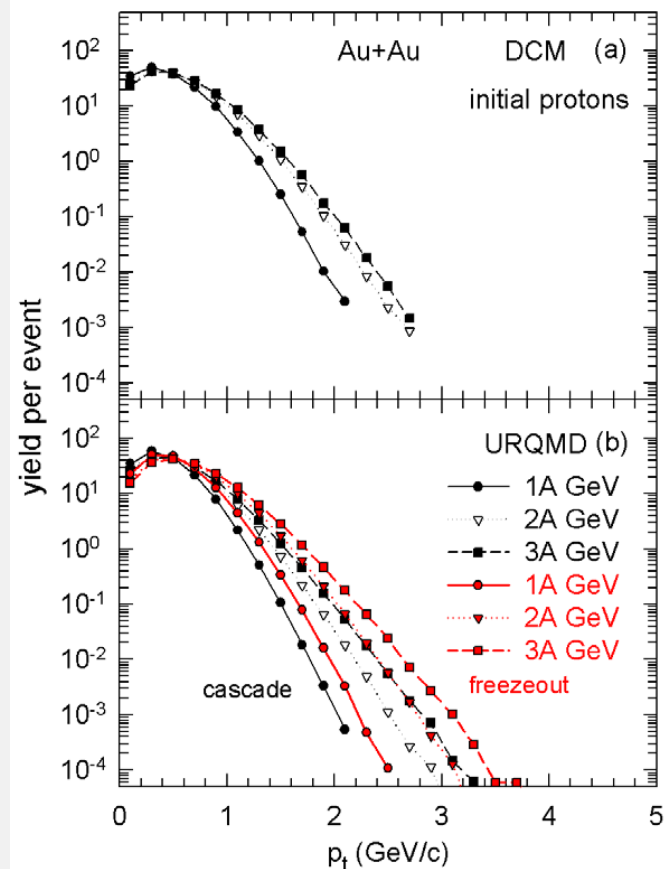
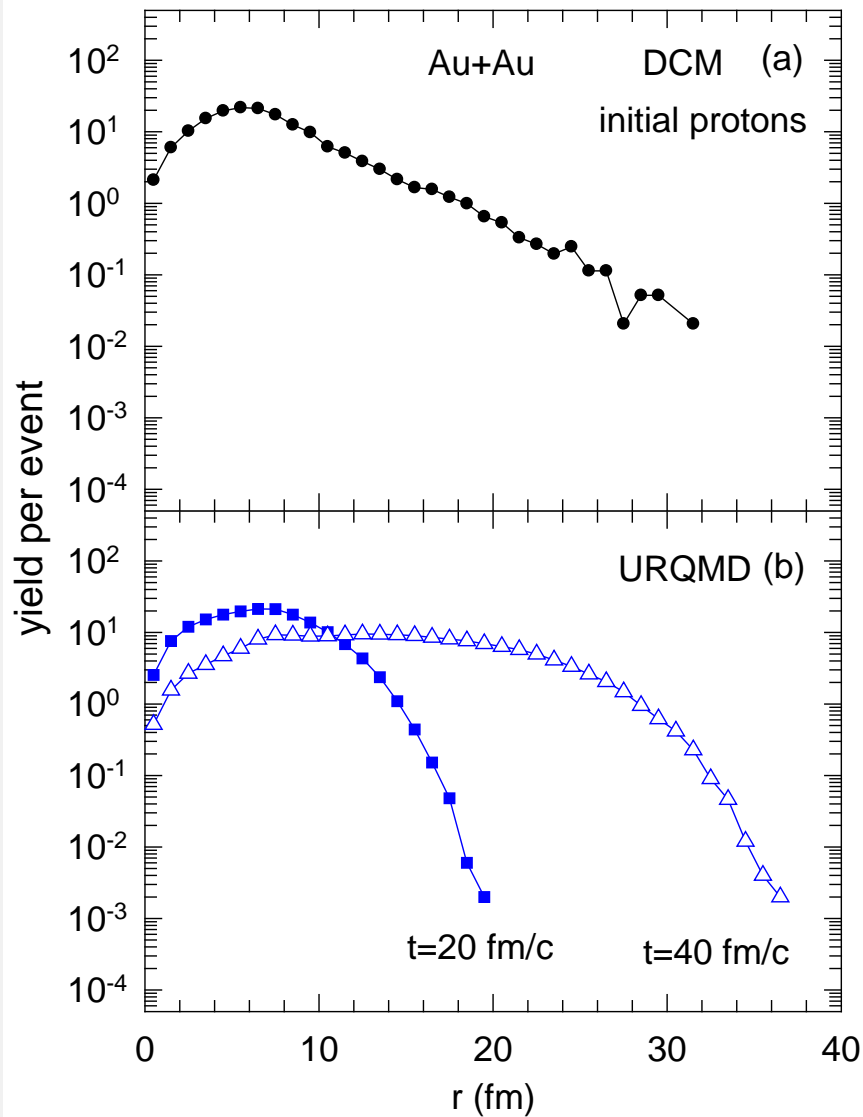
Phys.Rev.C103 (2021) 064602 + Phys.Rev.C106 (2022) 014607

Besides UrQMD the dynamical stage is simulated with the phase space generation (PSG) . They provide very different momenta distributions of baryons which cover the most important limits expected after this stage.

Selection of primary clusters (at low freeze-out density) by using the clusterization of baryon (CB) model (**Phys. Lett. B742, 7 (2015)**): according to their velocities $| \mathbf{V}_i - \mathbf{V}_0 | \leq \mathbf{V}_c$ and coordinates $| \mathbf{X}_i - \mathbf{X}_0 | \leq \mathbf{X}_c$.

Statistical formation of nuclei inside these clusters with SMM: de-excitation of the excited clusters. The excitation energy (or local temperature) of such clusters is important characteristics for the nuclear matter corresponding to coexistence region of NLGPhT.

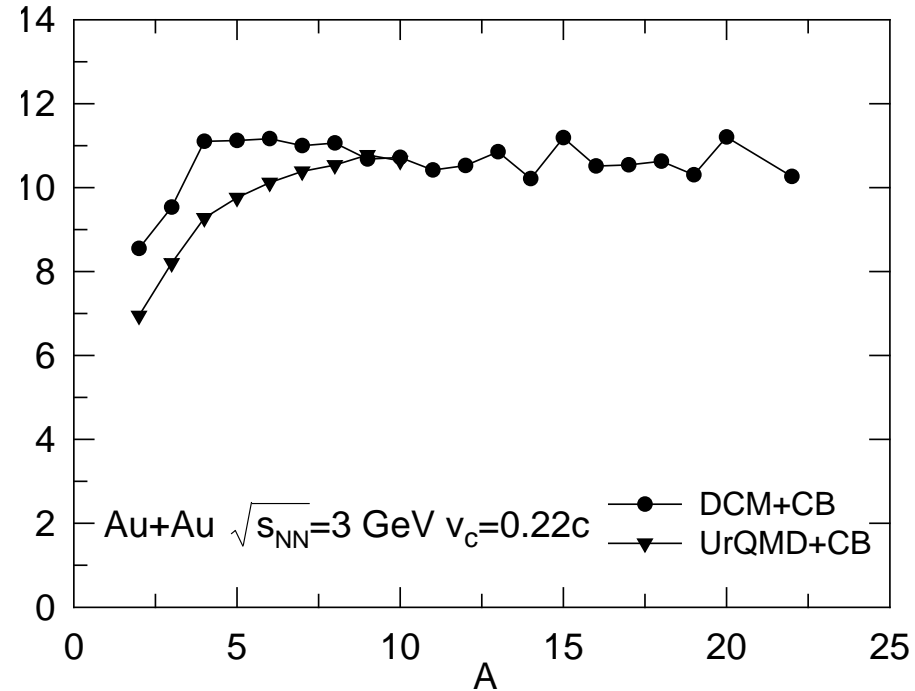
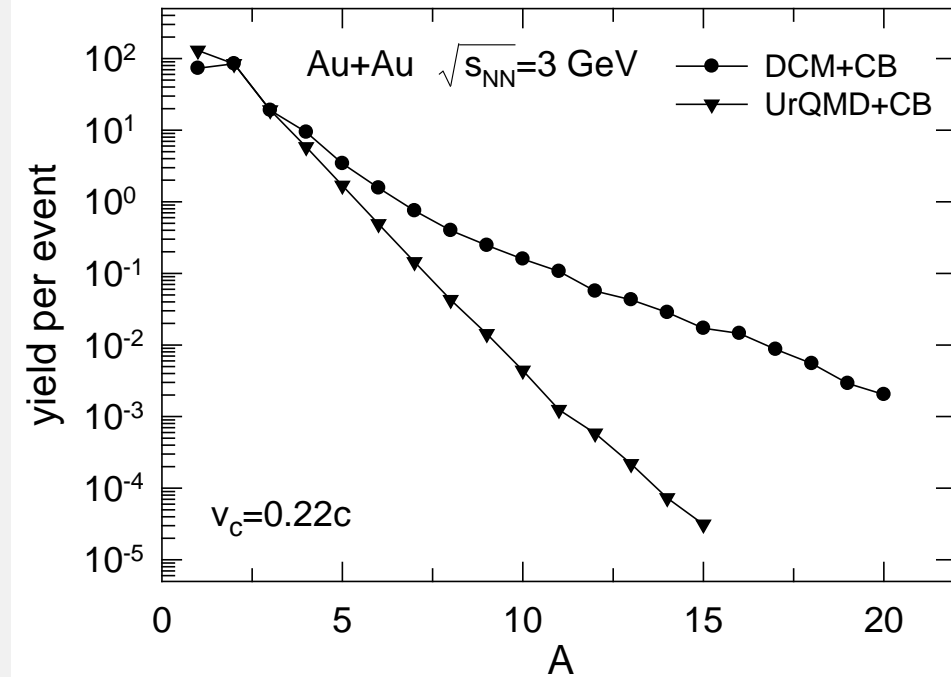
Construction of initial conditions for baryons in dynamical processes



hot baryon clusters

Mass distributions

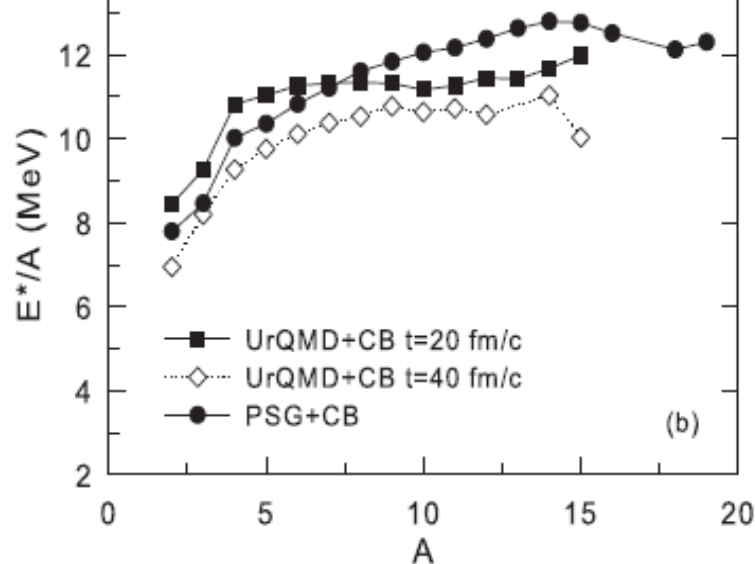
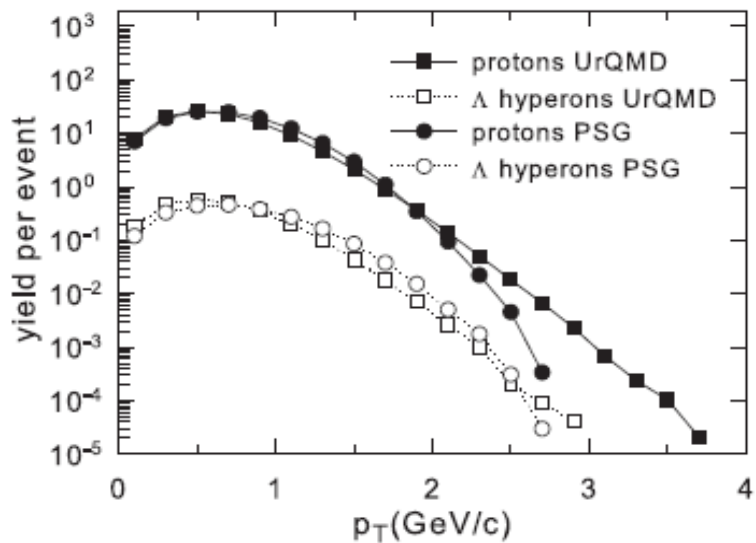
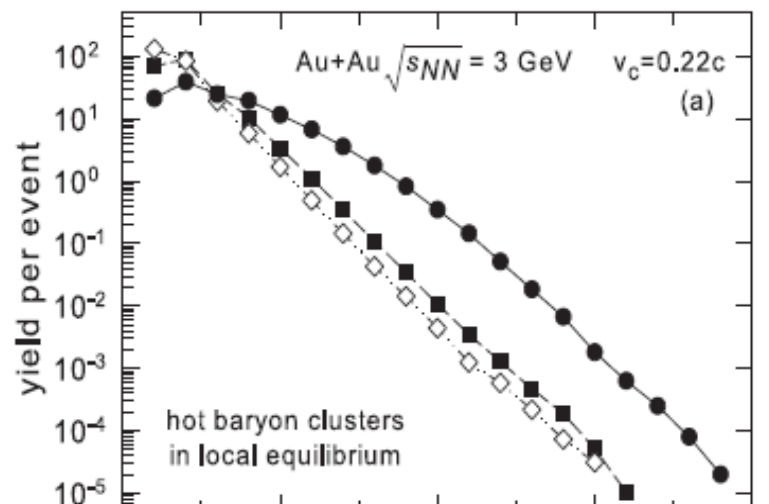
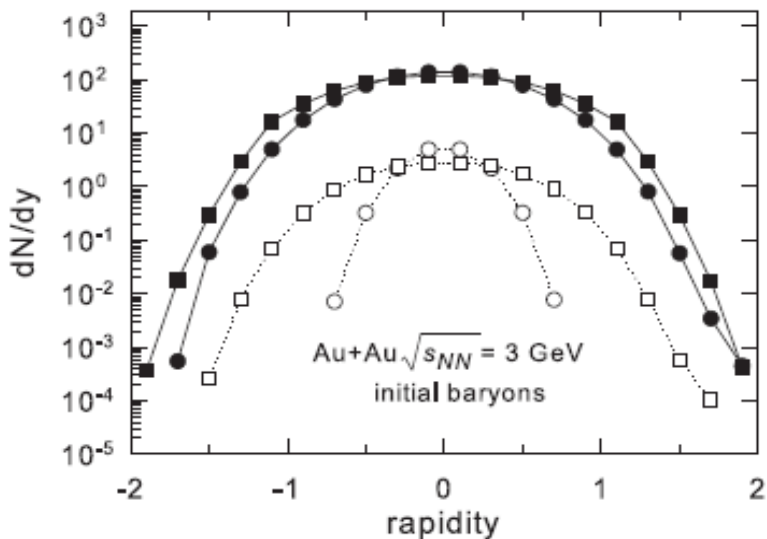
Excitation energies



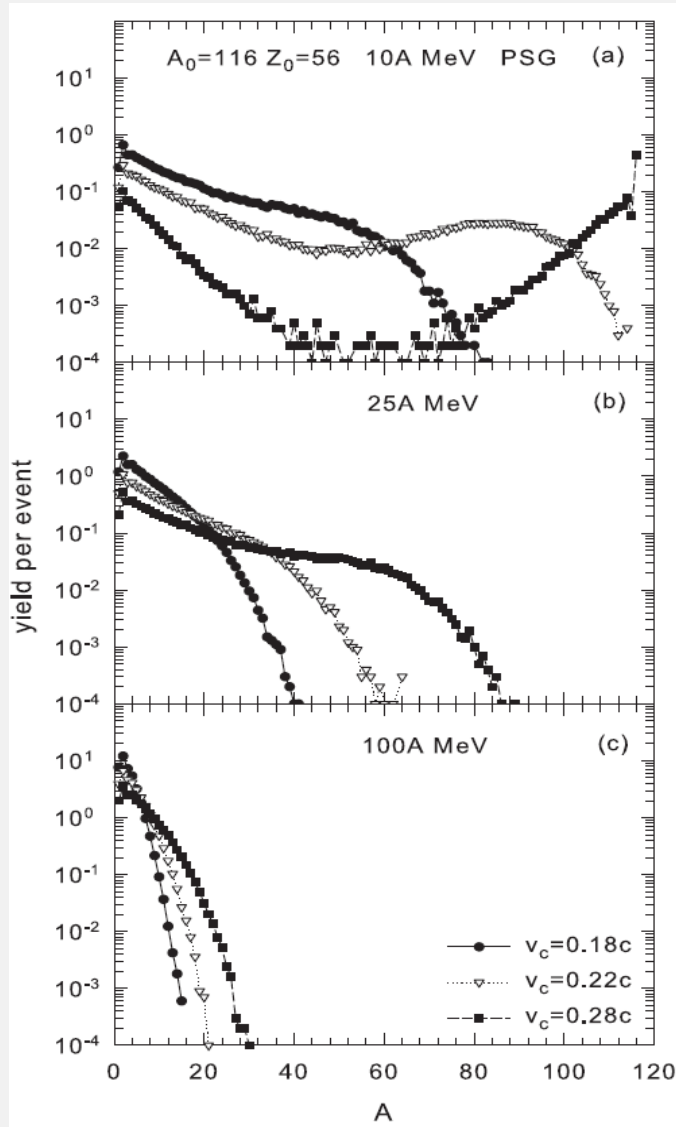
The calculations are performed with the UrQMD and DCM to generate baryons in central Au+Au collisions, $v_c = 0.22c$ is applied for the identification of hot clusters.

Baryon distributions (UrQMD and PSG) and baryonic clusters (CB) calculated for central collisions Au + Au at 3A GeV

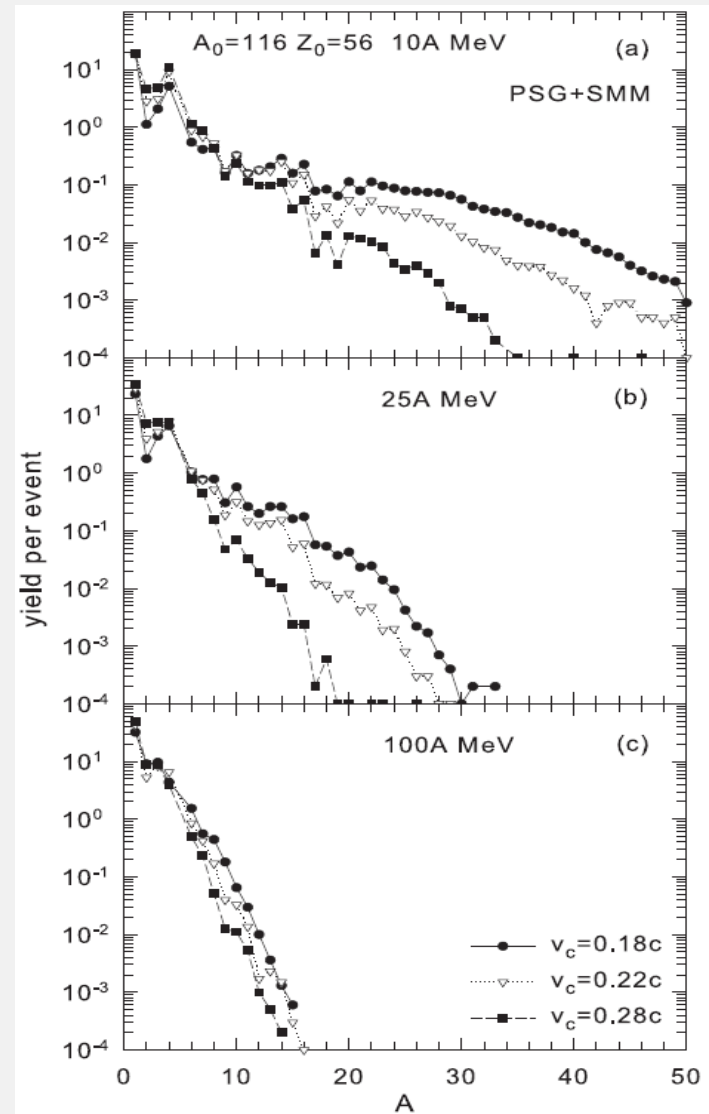
N. Buyukcizmeci, T.Reichert, A.S.Botvina, M. Bleicher, arXiv:2410.17449



Nuclear system consists of primary clusters in local equilibrium:

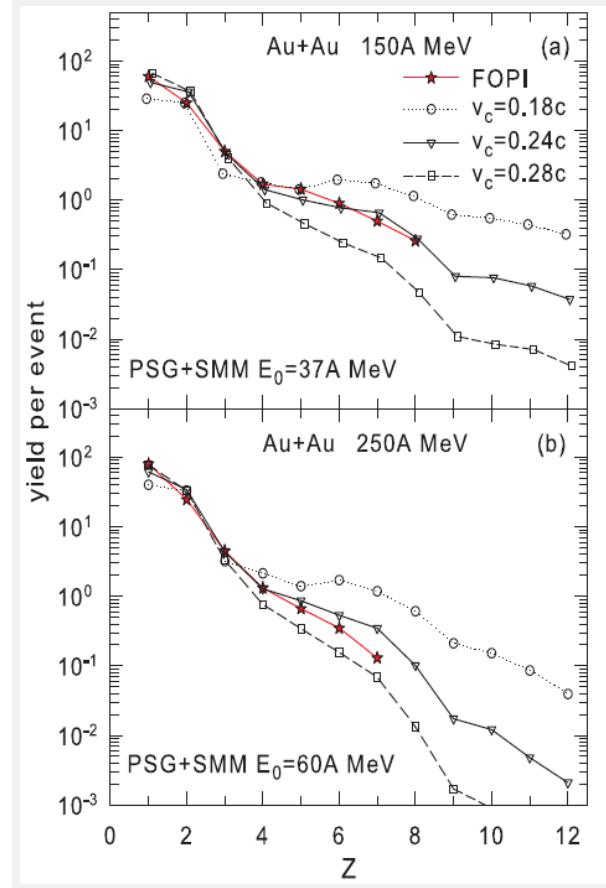
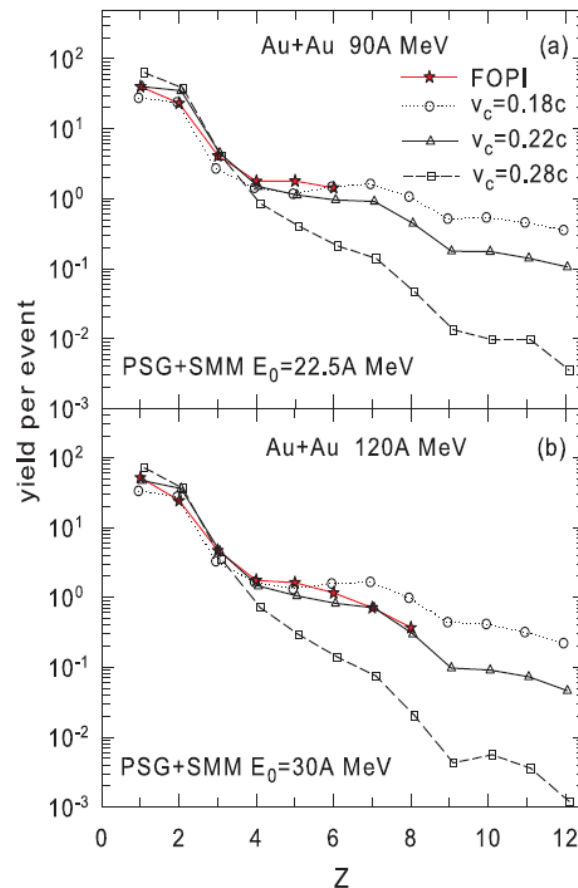
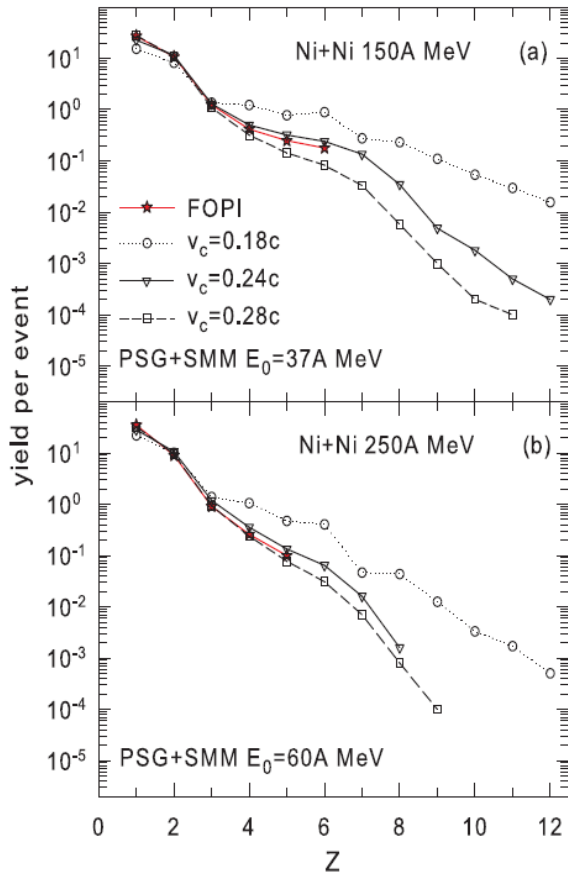


final nuclei after the statistical nucleation (disintegration of the excited clusters via SMM):



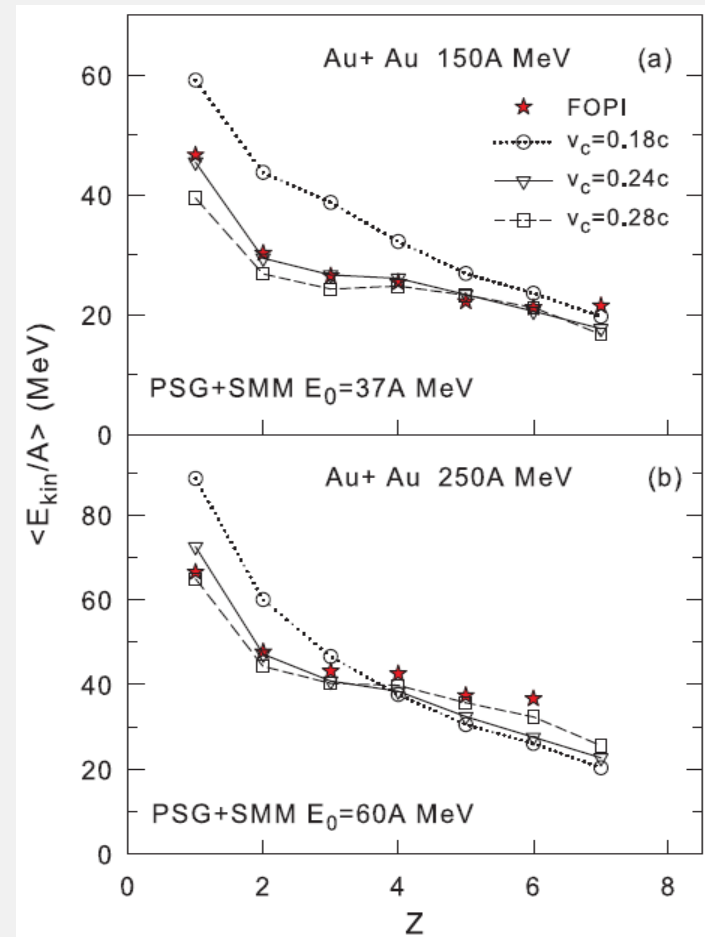
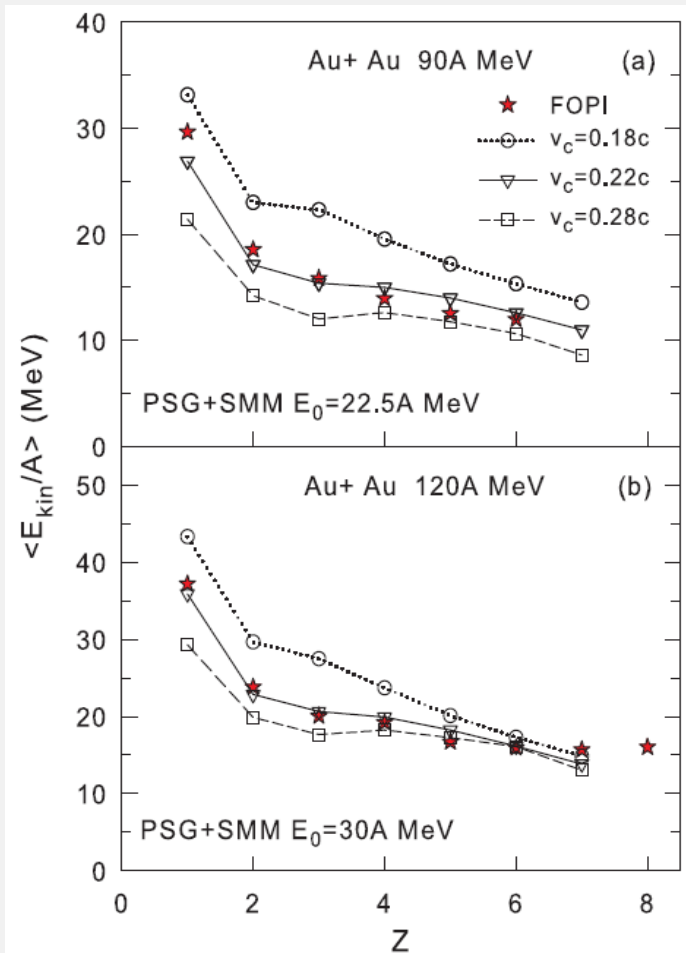
For the first, the consistent comparison with FOPI@GSI experimental data - Nucl. Phys. A848(2010)366 - on fragment production in central HI collisions is performed: Both charge yields and flow energies. Phys.Rev.C103(2021)064602 and Phys.Rev.C106(2022)1014607

yields of nuclei in different reactions:



(until now the production of nuclei ($Z > 2$) in central collisions was not possible to describe consistently under assumption of global chemical equilibrium)

kinetic energies of nuclei in different reactions:

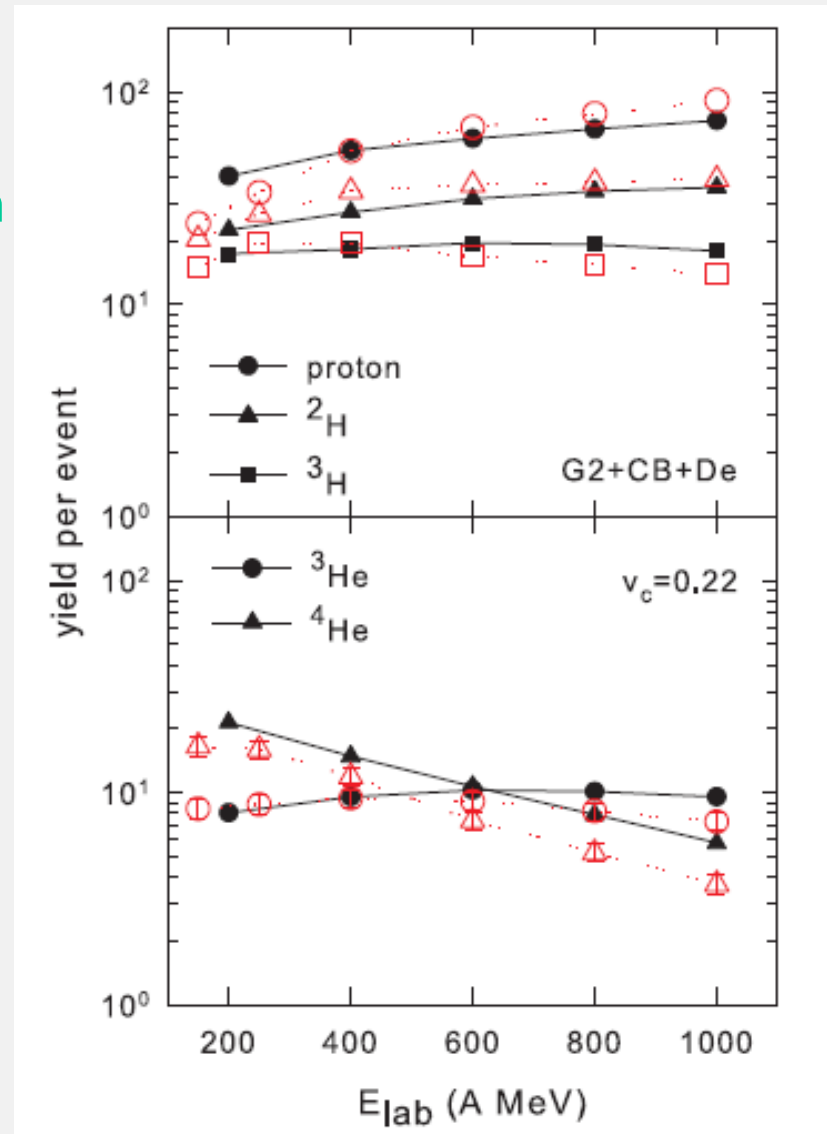


Important beam energy dependence of the light nuclei yields in Au+Au relativistic central collisions can be explained within our approach too.

Note: in simplistic coalescence picture yields of ^3He are larger than ^4He yields at all energies.
FOPI experimental data (red symbols) show intersection with increasing energy.

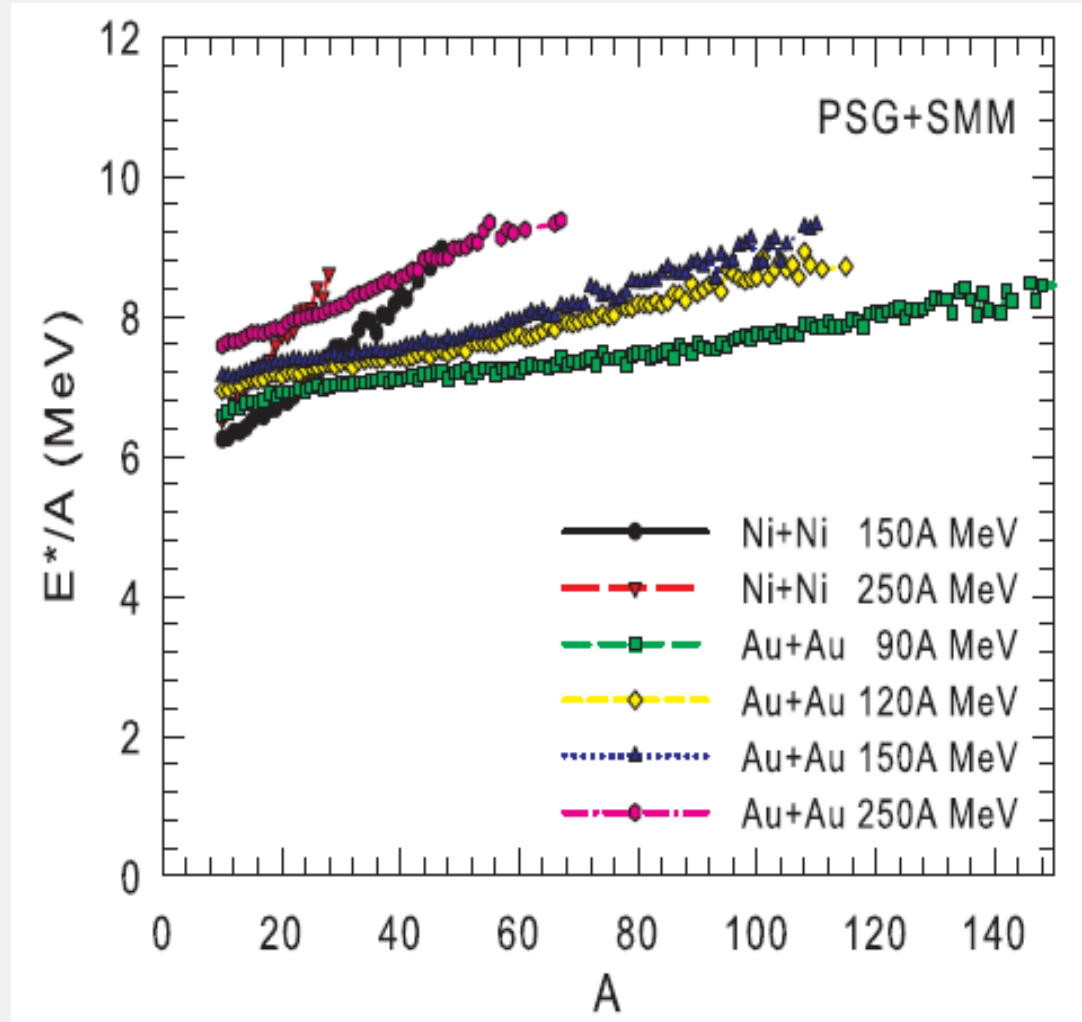
Relative behavior of yields of ^3He and ^4He with energy is important confirmation of the nucleation via decay of local statistical sources

Phys.Rev.C103 (2021) 064602



However, the description is possible if there is a limit for the excitation energy of the clusters: 6–10 MeV/nucleon, close to their binding energies. Temperature $T=6\text{--}8$ MeV (according to the statistical model) which corresponds to the coexistence region of the liquid-gas type phase transition in nuclear matter.

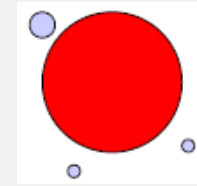
We may speak about an universal mechanism for nuclei formation both in peripheral and central heavy-ion collisions, independently on the way how the low density matter is produced: by thermal-like expansion of the excited residues (peripheral col.) or by dynamical-like expansion (central col.)



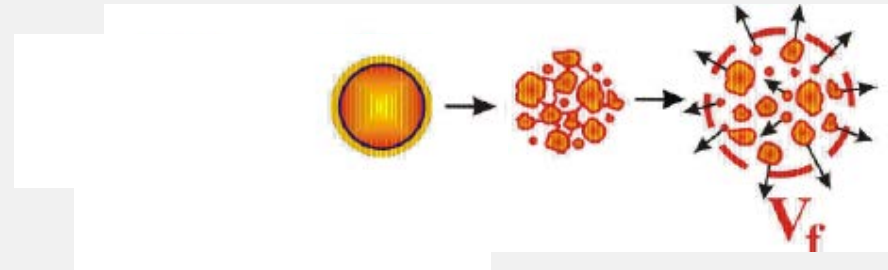
Conclusion on the nuclei production (disintegration of excited nuclei, or nucleation of individual baryons) described with the statistical approach:

Evolution of the statistical mechanism toward highly excited finite nuclear systems -

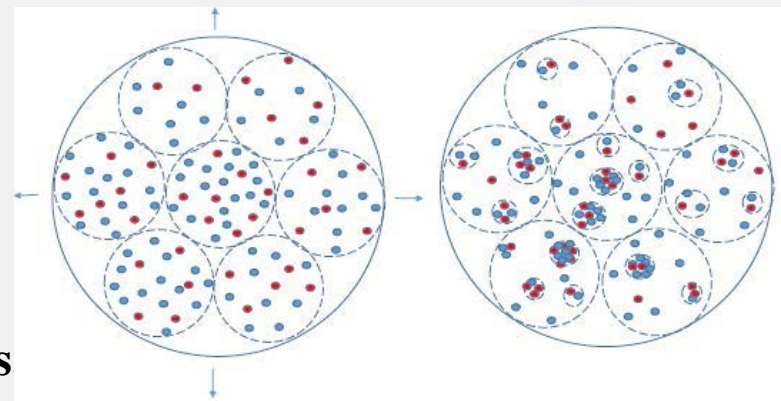
Compound nucleus conception –
excitation energies from 0 to 2-3 MeV/nucleon



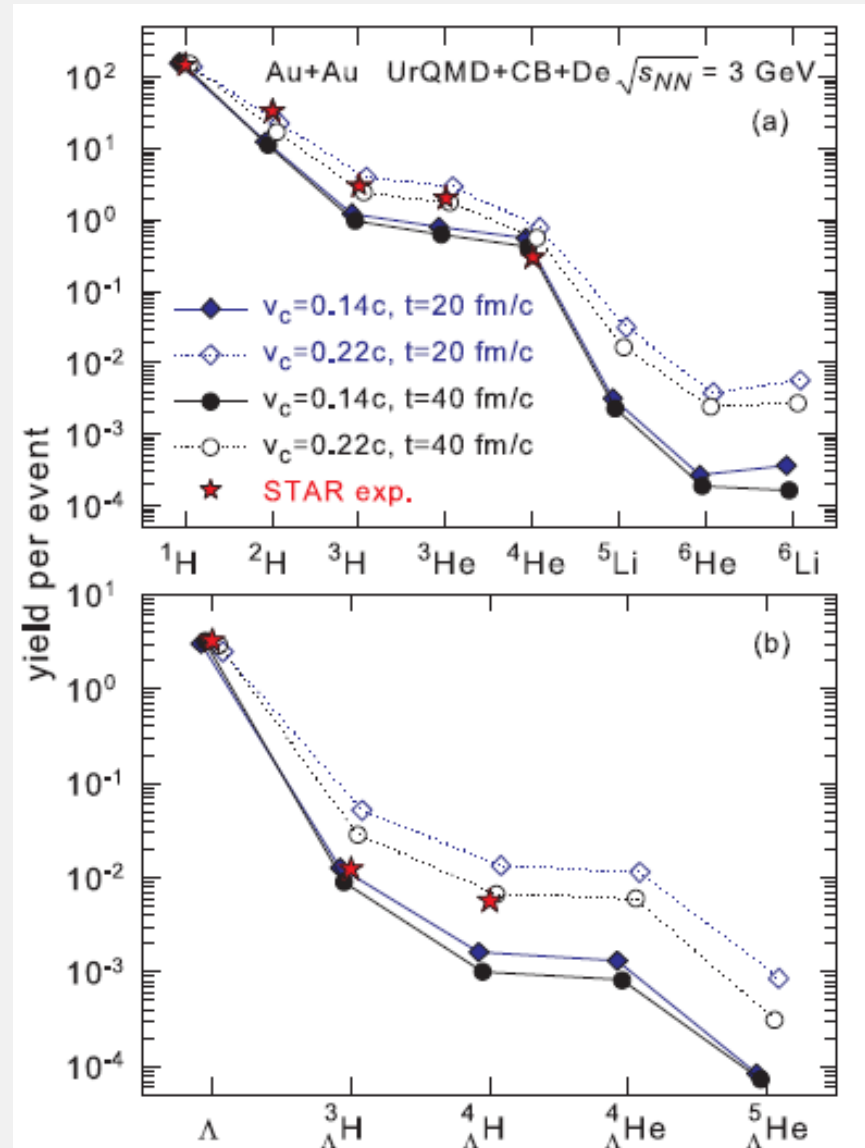
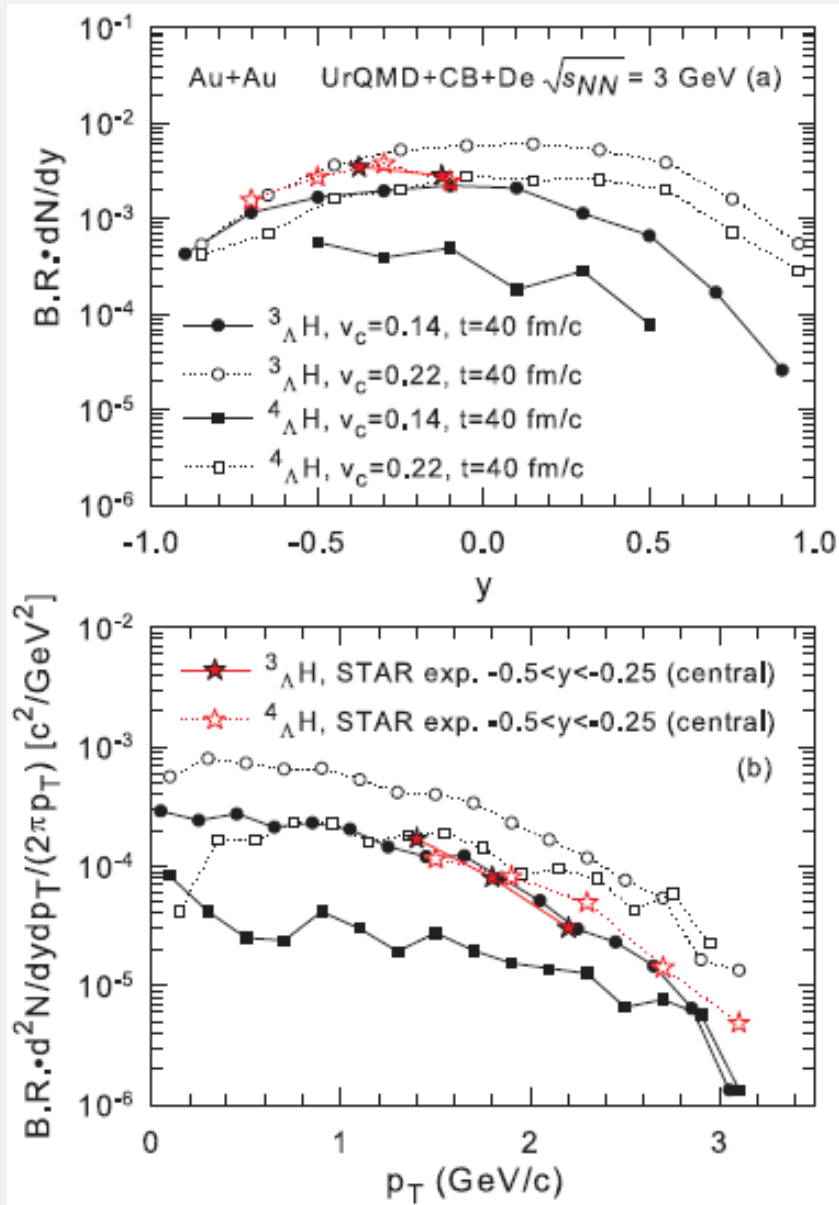
Freeze-out volume conception –
excitation energies from 2-3 to
around 8-10 MeV/nucleon



At energies more than 8-10 MeV/nucleon –
fragmentation of the expanding nuclear
matter at low density into locally
equilibrated clusters with moderate
energies (around 8-10 MeV/nucleon) and
nucleation (**nucleosynthesis**) in such clusters



Hypernuclei yields in central collisions (Au+Au, 3A GeV) - comparison with STAR experiment (PRL,128(2022)202301): PRC, 108, 054904 (2023)

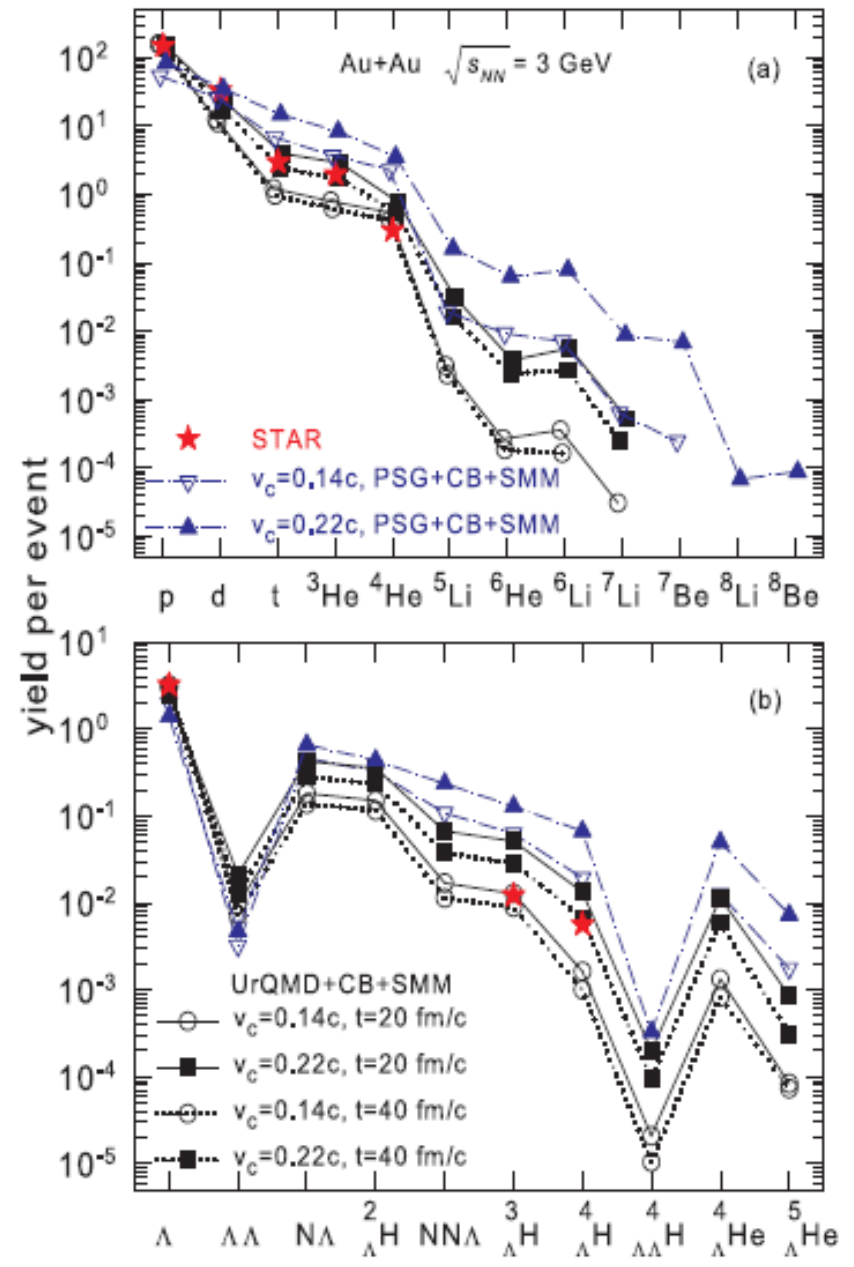


Advantage of relativistic HI collisions:
 Abundant yield of exotics and double
 strange hypernuclei: $N\Lambda$, $\Lambda\Lambda$
 (H-dibaryons) and others, which are
 difficult to produce in conventional
 hypernuclear experiments,

**HI collisions produce hypermatter
 and allow for the investigation of the
 hyperon and nucleon interaction:**
 There is a hyper-nucleosynthesis at
 low (subnuclear) density.

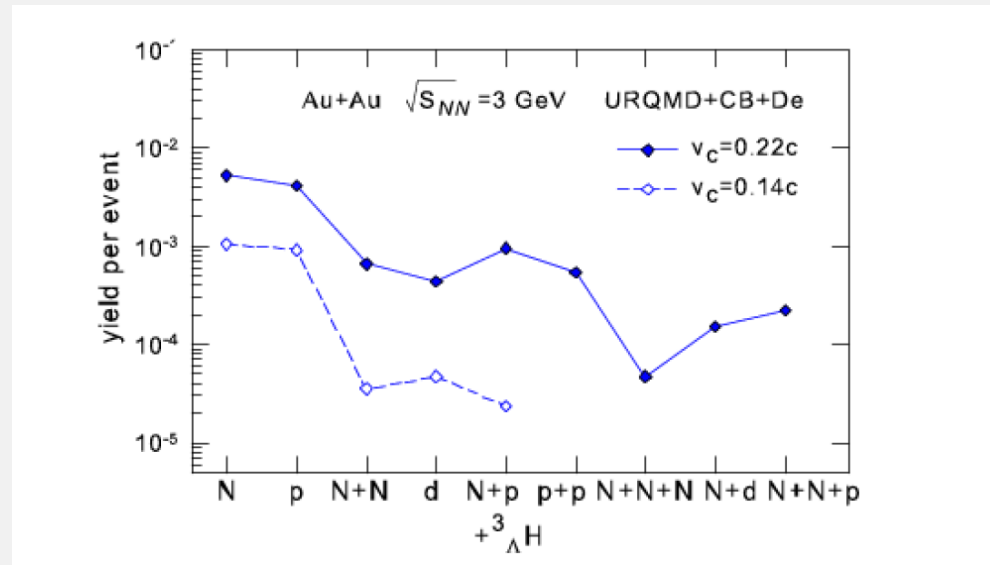
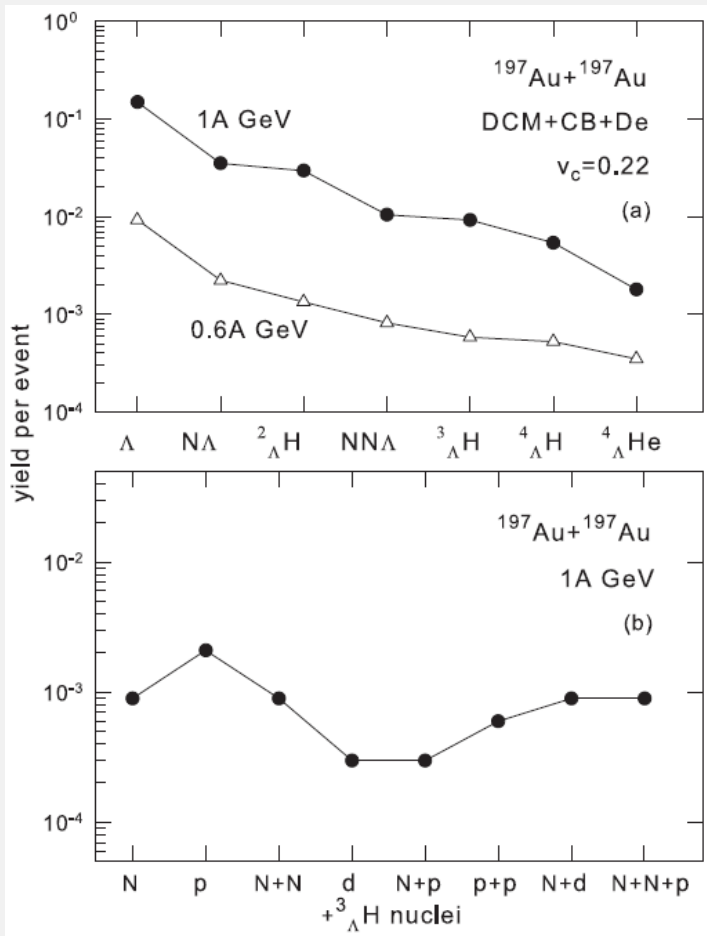
**Correlations between particle are
 necessary to measure, to reveal the
 nucleation mechanism.**

N. Buyukcizmeci, T.Reichert, A.S.Botvina, M. Bleicher
 arXiv:2410.17449



Production of hypernuclei in HI central collisions (GSI energy)

We can predict the hypernuclei yields in relativistic central collisions too. Many different light hypernuclei can be produced. The correlations between nuclear species exist and it can be used for their identification.



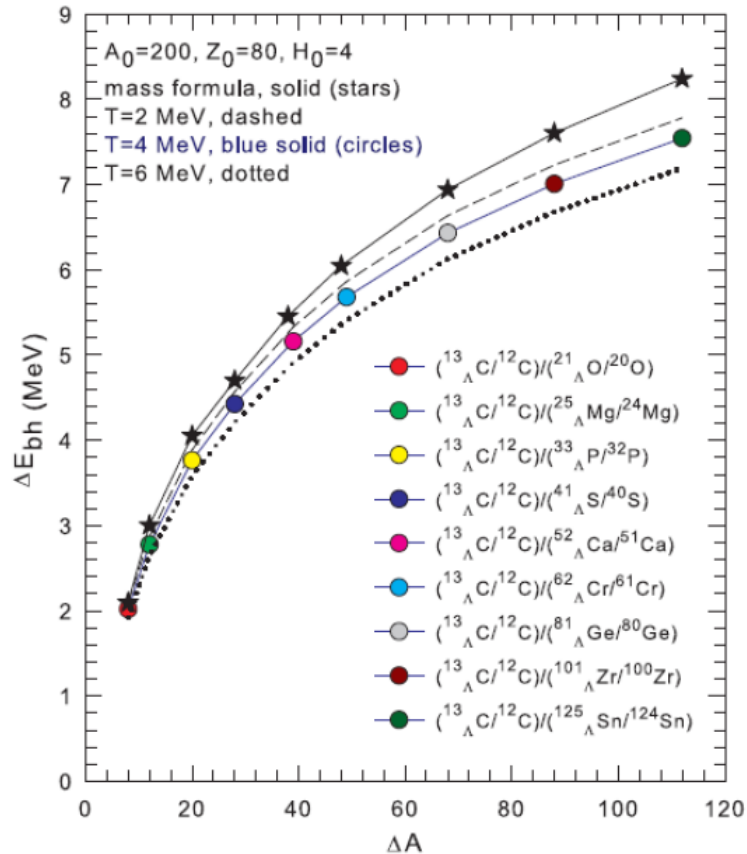
Statistical reaction models can be used not only for the production prediction:

Experimental yields of isotopes can be used for extracting properties of exotic cluster, e.g., the hyperon binding energies

Double ratio method :

$$\Delta E_{bh} \text{ vs } \Delta A$$

difference of hyperon energies in hyper-nuclei:
 Phys.Rev.C98(2018)064603



$$\Delta E_{bh} = T \cdot \left[\ln \left(\frac{(g_{A_1, Z_1, H} / g_{A_1-1, Z_1, H-1}) \cdot (A_1^{3/2} / (A_1 - 1)^{3/2})}{(g_{A_2, Z_2, H} / g_{A_2-1, Z_2, H-1}) \cdot (A_2^{3/2} / (A_2 - 1)^{3/2})} \right) - \ln \left(\frac{Y_{A_1, Z_1, H} / Y_{A_1-1, Z_1, H-1}}{Y_{A_2, Z_2, H} / Y_{A_2-1, Z_2, H-1}} \right) \right]$$

Tübitak 118F111

Properties of hypernuclei (hyperon binding) can be addressed in novel way!
 Future plans... UrQMD+CB+De

Conclusions

Collisions of relativistic ions are promising reactions leading to the nucleosynthesis of nuclei, exotic clusters with very different isospin, including hypernuclei. One can describe the process via the dynamical production of baryons and statistical nucleosynthesis.

Mechanisms of formation of hypernuclei in reactions: Strange baryons (Λ , Σ , Ξ , ...) produced in particle collisions can be transported to the spectator residues and captured in nuclear matter. Another mechanism is the nucleation of baryons at subnuclear density. It leads to light clusters and is effective at all rapidities.

Novel mechanism: The matter is subdivided into excited baryon clusters in local equilibrium and after the cluster decay the nuclei and hypernuclei of all sizes (and isospin), including short-lived weakly-bound states, multi-strange nuclei can be produced.

Advantages over other reactions: there is no limit on sizes and isotope content of produced exotic nuclei; probability of their formation may be high; a large strangeness can be deposited in nuclei.